CNWRA *A center of excellence in earth sciences and engineering*

A Division of Southwest Research Institute™
6220 Culebra Road • San Antonio, Texas, U.S.A. 78228-5166
(210) 522-5160 • Fax (210) 522-5155

April 13, 2001
Contract No. NRC–02–97–009
Account No. 20.01402.871

U.S. Nuclear Regulatory Commission
ATTN: Dr. John W. Bradbury
Division of Waste Management
Two White Flint North
Mail Stop TD–13
Washington, DC 20555

Subject: Transmittal of the deliverable "The Role of Radionuclide Sorption in High-Level Waste Performance Assessment—Journal Paper" (IM 01402.871.120).

Dear Dr. Bradbury:

The enclosed manuscript is identified as IM 01402.871.120 in the CNWRA Operations Plans for the Key Technical Issue (KTI) on Radionuclide Transport. The proposed title for this manuscript is "The Role of Radionuclide Sorption in High-Level Waste Performance Assessment: Approaches for the Abstraction of Detailed Models." This manuscript will be submitted for publication in a Soil Science Society of America proceedings volume entitled Soil Geochemical Processes of Radionuclides

The U.S. Department of Energy has identified radionuclide transport in the unsaturated and saturated zones as principal factors in the postclosure performance of the proposed repository at Yucca Mountain, Nevada. Sorption is an important aspect of how transport is modeled for high-level waste (HLW) performance assessment (PA). This manuscript presents background programmatic information, describes the role of sorption in PA in the HLW program, and presents two approaches to incorporate the key aspects of detailed sorption models in PA model abstractions. The manuscript describes key geochemical parameters controlling sorption and develops methods for using site-specific information to constrain transport parameters. Sensitivity analyses using the NRC Total System Performance Assessment code are also presented. This manuscript is based upon earlier technical work and reports conducted and prepared by the CNWRA for the NRC. Publication of this material serves in part to convey to the public the technical bases for NRC work in this area and contributes to the NRC strategic goal of increasing public confidence.

Washington Office • Twinbrook Metro Plaza #210
12300 Twinbrook Parkway • Rockville, Maryland 20852-1606

The manuscript is due at the volume editors by April 30, and programmatic approval prior to this date is desired. If you have any questions regarding this submittal, please contact me (210.522.5540) or Dr. David Turner (210.522.2139).

Sincerely yours,

Randall W. Fedors
for

English C. Pearcy, Element Manager
Geohydrology and Geochemistry

ECP:ar
d:gh&gc-fiscal\year-2001\letters\bradbury\the role of radionuclide....

cc:
J. Linehan
B. Meehan
D. DeMarco
E. Whitt
J. Holonich
W. Reamer
K. Stablein
J. Ciocco
B. Leslie
W. Dam
W. Patrick
CNWRA Directors
CNWRA Element Managers
D. Turner

The Role of Radionuclide Sorption in High-Level Waste Performance Assessment: Approaches for the Abstraction of Detailed Models

David R. Turner, F. Paul Bertetti, and Roberto T. Pabalan. Center for Nuclear Waste Regulatory Analyses, Southwest Research Institute, 6220 Culebra Road, San Antonio, TX 78238-5166

INTRODUCTION

Many countries are currently investigating long-term geologic disposal of high-level nuclear waste (HLW) (National Research Council, 1999; Nuclear Energy Agency, 1998). In the United States HLW program, the Nuclear Waste Policy Act of 1982 (as amended 1987) charges the U.S. Department of Energy (DOE) with characterizing and evaluating Yucca Mountain, Nevada as a potential site for a geologic HLW repository. A multiple barrier approach that includes both engineered and natural barriers to radionuclide release is typically endorsed. In this approach, HLW (spent nuclear fuel, defense waste) is placed in engineered waste packages and placed in an underground mined repository. When the repository is full, the drifts are closed and the repository sealed. The engineered barriers (waste form, waste canister, backfill) are designed to provide waste isolation for an extended period of time. In addition to providing a suitable environment for the waste packages and other engineered barrier components, the geosphere surrounding the repository is expected to provide additional isolation to reduce exposure at receptor group locations. The conceptual model assumes that after failure of the engineered barrier, radionuclides are released and transported in the groundwater. Understanding the means by which radionuclides migrate in the subsurface is therefore a critical part of performance assessment (PA) calculations that attempt to assess the safety of the repository concept. Processes such as sorption that serve to reduce radionuclide concentrations or retard radionuclide migration are considered to be favorable to repository performance.

Experimental and modeling studies indicate that sorption behavior, and the sorption coefficient (K_d) that is used to describe it, is strongly dependent on solution and mineral properties along transport paths. Without an abundance of site-specific chemical and mineralogical data, it is difficult to extrapolate K_d values beyond experimental conditions with any quantifiable certainty in PA calculations. However, because experimental evidence indicates that K_ds vary in a systematic fashion that can be modeled using well-established geochemical approaches, there is an underlying link, dependent on variations in the chemistry of the system at Yucca Mountain, that may be used to correlate the sorption behavior of different radioelements. The purpose of this study is to outline an approach that incorporates aspects of detailed geochemical models in estimating sorption and radionuclide transport parameters for radionuclide transport at Yucca Mountain, and to describe how this approach may be implemented in PA. The focus is on identifying geochemical parameters that exert the most control on radionuclide sorption, and incorporating the effects of those parameters in a way that lends itself to the simplification (abstraction) process used in PA for the proposed repository. In this way, PA models can represent chemical effects on sorption behavior more accurately.

BACKGROUND

A number of countries are investigating geologic disposal of HLW, including the United States, Sweden, Finland, Germany, and Japan, (National Research Council, 1999; Nuclear Energy Agency,

1998). Although the details of the different national programs are different, there are many similarities. The following section provides a brief discussion of the HLW disposal program in the United States, the role of the different government agencies, and an outline of how PA is used in licensing decisions.

Introduction to the U.S. High-Level Nuclear Waste Management Program

The proposed site at Yucca Mountain is located approximately 175 km northwest of Las Vegas, Nevada (Figure 1). If the site is found to be suitable, approved and licensed, the repository would be located in a thick sequence of Tertiary volcanic tuffs. Although a number of basins have been identified in the region, groundwater flow through the area is generally from recharge areas to the north through a series of aquifers, including both tuffs and regional Paleozoic carbonates, with discharge from springs, seeps, and agricultural and domestic wells to the south of Yucca Mountain (Winograd and Thordarson, 1975). The proposed regulatory framework (U.S. Nuclear Regulatory Commission, 1999a) establishes criteria for repository performance. When finalized, these criteria will conform to the radiation protection standards established for Yucca Mountain by the U.S. Environmental Protection Agency (Environmental Protection Agency, 1999). Specifically, the quantitative measure of performance is based on radiation dose to a hypothetical critical group located about 20 km south (downgradient) from the proposed repository. The time period of interest to performance is 10,000 y after permanent closure.

In the United States HLW program, the DOE is the license applicant. The U.S. Nuclear Regulatory Commission (NRC) evaluates the DOE license application against its regulations. An important part of the proposed NRC regulations (10 CFR Part 63, U.S. Nuclear Regulatory Commission, 1999a) governing the licensing, construction, operation, and permanent closure of the proposed repository at Yucca Mountain is the use of PA calculations to evaluate the performance of the different barriers to waste containment and migration over long time periods (10 CFR 63.114). These PA analyses are intended to represent the degree of knowledge of the Yucca Mountain site, and at the same time, represent the uncertainty in both our conceptual and mathematical models of the site.

The Role of Total System Performance Assessment in HLW Management

The multiple barrier approach to geologic disposal of HLW at Yucca Mountain relies on the geologic setting to provide a degree of isolation in addition to that provided by the engineered barrier system for a period of 10,000 y or more. Complex coupled computer models have been developed to evaluate the suitability of Yucca Mountain through a series of site-specific PA calculations. In the DOE program, these PA calculations are carried out under an iterative series of Total System Performance Assessments (TSPA) that are updated as site characterization proceeds and repository design evolves (Civilian Radioactive Waste Management System, Management and Operating Contractor, 1998, 2000a; U.S. Department of Energy, 1998). The NRC also has developed an independent capability in PA, including the Iterative Performance Assessment (IPA) (Wescott et al., 1995) and Total-system Performance Assessment (TPA) (U.S. Nuclear Regulatory Commission 1999b,c).

In the DOE Repository Safety Strategy (Civilian Radioactive Waste Management System, Management and Operating Contractor, 2000b), a fundamental quantity of interest in TSPA calculations is the rate of radionuclide transport from the proposed repository through the subsurface to the biosphere and potential receptor groups. Reduction in radionuclide concentrations and delay in arrival times during radionuclide transport are identified by the DOE as key attributes that need to be tested in any suitability

demonstration for the proposed repository at Yucca Mountain. As part of the geological setting, sorption processes can retard radionuclide transport, delaying arrival times at the receptor group location(s), and can reduce radionuclide concentrations at the point of exposure.

TSPA calculations for the natural barrier system at Yucca Mountain require linking a number of geological, geochemical, and hydrological models. Because of the long simulation period and the heterogeneous geochemical and hydrological systems at Yucca Mountain, simplification of complex process models is necessary to reduce the computational burden for PA calculations. In PA, the process of simplification is called model abstraction. Sorption modeling is an example where detailed geochemical models are available for simulating reactive transport (e.g., Yeh and Tripathi, 1989, 1991), but are not suited for incorporation in the current generation of PA codes.

During the abstraction process, critical aspects controlling a given process are identified, conceptual models are developed, parameters are defined, and uncertainties estimated. The PA abstraction is supported by a combination of site and laboratory data, more detailed process models, and in some cases expert judgement (Figure 2). The purpose of this study is to outline approaches that can be used to abstract the results from geochemical sorption models for use in PA.

Overview of the Role of Radionuclide Sorption in the Yucca Mountain TSPA

One of the initial reasons for proposing Yucca Mountain as a location for the repository is the existence of a deep regional water table. The proposed repository will be located some 250 m below the ground surface and approximately 300 m above the regional water table (Civilian Radioactive Waste Management System, Management and Operating Contractor, 2000a,c). Geologic HLW disposal at Yucca Mountain is unique in this respect, in that the repository would be located in the unsaturated zone under oxidizing conditions. Conceptual models of the proposed Yucca Mountain repository include vertical transport through fractures and matrix in the volcanic tuff of the unsaturated zone followed by lateral transport through the saturated zone to the receptor location. The first part of the saturated zone transport leg is anticipated to be through fractured volcanic tuff, with the last part of the transport through saturated alluvium. There is some current uncertainty in the length of the flow path through the alluvium, and this is treated as a sampled parameter in the DOE TSPA.

The DOE has been conducting TSPA analyses of the proposed repository at Yucca Mountain since 1991. As considered in TSPA, sorption is a general term for describing a combination of chemical interactions between the dissolved radionuclides and the solid phases (Civilian Radioactive Waste Management System, Management and Operating Contractor, 2000a). Sorption, characterized by a single K_d value, reduces the rate of radionuclide advective transport and amplifies the effects of matrix diffusion through its potential effect on increasing concentration gradients. This 'lumped' approach of incorporating all potential retardation mechanisms in a single K_d is readily incorporated into existing transport codes and simplifies the numerical simulation of radionuclide migration. It does not, however, distinguish between different sorption processes and geochemical interactions, such as surface adsorption, precipitation, and ion exchange.

Batch sorption experiments are used to identify the overall partitioning between the aqueous and solid phase, and establish limits on K_d. The magnitude of K_d is a function of the chemical element, the rock type involved in the interaction, and the geochemical conditions of the water contacting the rock. In

PA calculations, K_d is considered to be an uncertain parameter. The uncertainty is defined using a probability distribution function (PDF) that places upper and lower limits on K_d and, if possible, identifies the central tendency of the PDF. The PDFs are sampled to obtain multiple realizations to generate a family of Complementary Cumulative Distribution Functions (CCDF) for radionuclide release (Wilson et al., 1994). Because it is impractical to perform batch experiments under all anticipated conditions, the PDFs are typically developed either formally or informally by a group of one or more experts who consider the sorption behavior of the critical radionuclides and the anticipated variability in water and mineral chemistry over the transport path. During TSPA calculations, each PDF is sampled in multiple realizations that are used to generate statistics of the estimated dose to the receptor group(s) (Civilian Radioactive Waste Management System, Management and Operating Contractor, 2000a; U.S. Nuclear Regulatory Commission, 1999b,c).

The approach outlined above has been applied to modeling radionuclide sorption in the porous matrix and alluvium at Yucca Mountain. In the DOE TSPA analyses, eight radioelements are transported through four basic types of hydrostratigraphic units at Yucca Mountain: devitrified tuff, vitric tuff, zeolitic tuff, and alluvium (Civilian Radioactive Waste Management System, Management and Operating Contractor, 2000a). Each rock type or hydrostratigraphic unit is assigned a K_d PDF for each radionuclide of interest. The NRC TPA analyses track 16 radioelements through eight separate hydrostratigraphic units (U.S. Nuclear Regulatory Commission, 1999b,c). This approach rapidly leads to a large number of parameters for sorption and transport in the matrix. In TSPA simulations, it is assumed that each sampled K_d value is constant for a given hydrostratigraphic unit and over the entire time. It is further assumed in the sampling procedures used in some PA models (Civilian Radioactive Waste Management System, Management and Operating Contractor, 2000a,b,c; U.S. Nuclear Regulatory Commission, 1999b,c) that the sorption parameters for the radionuclides of concern are statistically independent of one another.

The amount of retardation that sorption in the matrix contributes under actual transport conditions is a function of both K_d and the transport paths. For example, in the DOE TSPA analyses, the majority of the flow is through fractures in the devitrified tuff, and flow tends to bypass the zeolitic tuff because of its low permeability (Civilian Radioactive Waste Management System, Management and Operating Contractor, 2000a,b,c). Sorption is most effective in the vitric tuff and its effectiveness in the devitrified tuff is tied to the degree to which matrix diffusion moves radionuclides out of fractures and into the rock matrix where there are assumed to be more available sorption sites.

Sorption is also a potential retardation mechanism for radionuclide transport through fractures. The surfaces of fractures are often lined with minerals that may be capable of sorbing some of the radionuclides; however, there is limited characterization of the extent and distribution of fracture-lining minerals along potential flow paths (Carlos et al., 1995). In the conceptual model used for Yucca Mountain, it is conservatively assumed that there is no sorption (i.e., $K_d = 0$) in fractured tuff for radionuclides being tracked in PA (Civilian Radioactive Waste Management System, Management and Operating Contractor, 2000a,b,c; U.S. Nuclear Regulatory Commission, 1999b,c).

Both the DOE and the NRC use sensitivity analyses to examine the importance of sorption to repository performance (Civilian Radioactive Waste Management System, Management and Operating Contractor, 1998; U.S. Nuclear Regulatory Commission, 1999b,c). Although the specific results vary, the most significant radionuclides contributing to dose typically includes radionuclides such as ^{99}Tc, ^{129}I, and sorbing ^{237}Np that are anticipated to be highly soluble and weakly sorbing under the geochemical

conditions expected at Yucca Mountain. Other radionuclides are predicted to be important either due to colloid transport, high inventory, or a high dose-conversion factor (^{239}Pu, ^{241}Am, ^{238}U, and ^{230}Th) (Civilian Radioactive Waste Management System, Management and Operating Contractor, 1998).

RADIONUCLIDE SORPTION BEHAVIOR

Improving the ability to address the geochemical controls on sorption in PA abstractions depends on understanding the key parameters controlling radionuclide sorption behavior. The approaches outlined below are focused on actinides (U, Np, Pu, Th, Am), but can be applied to other radionuclides of interest in PA.

Key Geochemical Parameters—Actinides

The distribution (or sorption) coefficient (K_d) is a convenient empirical ratio for representing batch sorption data and is commonly used in transport models in PA. The K_d ($mL \cdot g^{-1}$) can be defined as:

$$K_d\ (mL \times g^{-1}) = \frac{\text{equilibrium mass of radionuclide sorbed on solid}}{\text{equilibrium mass of radionuclide in solution}} \times \left(\frac{V}{M}\right) \qquad [1]$$

where V is the volume of experimental solution in mL and M is the mass of solid in g. The use of K_d normalizes sorption data to the solid-mass to solution-volume (M/V) ratio used in laboratory batch experiments and provides a means of accounting for the change in solution concentration that occurs during the course of the experiment.

For actinides, sorption behavior typically varies as a function of its aqueous speciation (Figure 3), with a close correspondence between the pH dependence of sorption behavior and the predominance field of actinide-hydroxy complexes (Bertetti et al., 1998; Pabalan et al., 1998). Under low pH conditions, actinide sorption tends to be weak, except under low ionic strength conditions for cation exchangers such as montmorillonite and, to a lesser extent, clinoptilolite (e.g., Zachara and McKinley, 1993; McKinley et al., 1995; Pabalan et al., 1993; Turner et al., 1996). With increasing pH, actinide sorption increases, with a maximum typically in the pH range where the hydroxy complexes are important. In carbonate-free laboratory systems, actinide sorption continues to increase with increasing pH and increasing hydrolysis (e.g., Allard et al., 1984; Hsi and Langmuir, 1985; McKinley et al., 1995; Turner et al., 1998). In addition to pH, actinide sorption behavior is also sensitive to the presence of carbonate or other ligands in solution that affect aqueous speciation (Figure 4). For example, in carbonate-bearing systems, actinide sorption tends to decrease with increasing pH and/or increasing carbonate concentration (Pabalan et al., 1998; Bertetti et al., 1998; Sanchez et al., 1985; LaFlamme and Murray, 1987).

In contrast to the relatively pronounced effects of aqueous speciation on actinide sorption, the similarity in the pH-dependence of actinide sorption on a wide variety of minerals such as quartz, α-alumina, clinoptilolite, montmorillonite, amorphous silica, kaolinite, and titanium oxide, suggests a relative insensitivity to surface charge characteristics of the sorbent as compared to the effect of changing the total number of available sites. For example, the data in Figure 3 demonstrate that U(VI) sorption on quartz, α-alumina, clinoptilolite and montmorillonite is strongly affected by solution pH (Pabalan et al., 1998). Although the minerals used in the experiments have different mineralogic and surface properties,

U(VI) sorption on these minerals is similar with respect to dependence on pH. In all cases, U sorption is at a maximum at near neutral pH (~6.0 to ~6.8) and decreases sharply towards more acidic or more alkaline conditions. The experimental and modeling results demonstrate that changing M/V has little influence on actinide sorption, except at low values. Ionic strength effects are limited for actinide surface complexation reactions, although these effects can be important if ion exchange is the predominant sorption mechanism.

Experimental sorption results are typically plotted in terms of percent sorbed versus pH (Figure 5a). In the U(VI)-H_2O-CO_2 system, the amount of U(VI) sorbed (in percent) relative to the initial amount of U(VI) in solution increases with increasing M/V ratio, giving a broader sorption "envelope." The apparent M/V effect, however, is mostly eliminated if the results are plotted in terms of K_d (Figure 5b). As demonstrated in Pabalan et al. (1998), U(VI) sorption on quartz, α-alumina, clinoptilolite, and montmorillonite is similar with respect to pH dependence. However, the K_d values for the different minerals vary over three orders of magnitude. This variation is an artifact of normalizing the data to the sorbent mass and representing sorption data in terms of K_d.

Surface areas measured by gas adsorption (e.g., N_2-BET) methods are a relative index of the number of sorption sites on the mineral surface and it may be more useful to represent sorption data normalized to the specific surface area of the mineral sorbent (Bertetti et al., 1998; Pabalan et al., 1998; Smith and Schafer, 1999). Figure 6(a) presents the results of U(VI) sorption on quartz, α-alumina, clinoptilolite, and montmorillonite, plotted in terms of K_d. In contrast, Figure 6(b) presents the same U(VI) sorption data replotted in terms of K_a ($mL \cdot m^{-2}$), where K_a is K_d normalized to the mineral's N_2-BET specific surface area (S_a, $m^2 \cdot g^{-1}$) (i.e., $K_a = K_d/S_a$). As shown in Figure 6(b), surface area normalized sorption data for clinoptilolite and montmorillonite are indistinguishable, whereas surface area normalized sorption data for quartz and α-alumina are almost coincident. The α-alumina K_a are lower than those of quartz due to the higher initial U concentration of the α-alumina experiments.

Surface areas determined by N_2-BET methods most likely overestimate the amount of sorption sites on layered silicates such as montmorillonite and zeolitic minerals such as clinoptilolite. For example, it is believed that surface complex formation of U(VI) on montmorillonite occurs on the hydroxylated edge sites of the mineral (Zachara and McKinley, 1993; Turner et al., 1996). Wanner et al. (1994) estimated that only 10% of the N_2-BET specific surface area is accounted for by the crystallite edges of montmorillonite. Assuming that the 'effective' surface area (S_{ea}) for montmorillonite and clinoptilolite is equivalent to about 10% of the measured S_a, sorption data for montmorillonite and clinoptilolite can be recast in terms of $K_{a'}$, where $K_{a'}$ is K_d normalized to the mineral's S_{ea} (i.e., $K_{a'} = K_d/S_{ea}$). For nonlayered and nonporous minerals such as quartz and α-alumina, $K_a = K_{a'}$. Figure 7 plots $K_{a'}$ values for quartz, clinoptilolite, and montmorillonite. As shown in the figure, U(VI) sorption on these minerals, which have distinct mineralogic and surface properties, are essentially equivalent when recast in terms of $K_{a'}$. This suggests that at least for aluminosilicate minerals, casting sorption in terms of $K_{a'}$ provides a generalized basis for PA transport calculations. The K_d values for a given hydrostratigraphic unit can then be backed out assuming an effective specific surface area. Similar results have been demonstrated for Np(V) (Bertetti et al., 1998). However, limited data and incomplete description of experimental conditions precludes examining these trends for all actinide-mineral systems of interest in HLW disposal. Therefore, an assumption underlying the approaches developed in this study is that other actinides will exhibit similar behavior.

Modeling Sorption Behavior—Surface Complexation Approaches

The pronounced effects of aqueous chemistry on actinide sorption behavior suggest that sorption modeling should account for changing physicochemical conditions. A number of different modeling approaches of varying complexity can be used to incorporate the effects of chemistry on radionuclide sorption. A class of models that has been used with success in modeling pH-dependent sorption for actinides and other metals is the electrostatic surface complexation model (SCM). These models are equilibrium representations of sorption at the mineral-water interface and are discussed in detail elsewhere (Dzombak and Morel, 1999; Davis and Kent, 1990; Serne et al., 1990; Hayes et al., 1991; Turner, 1995), with only a brief overview presented here.

Model Description

Applying SCMs requires assuming analogous behavior between aqueous speciation in the bulk solution away from the mineral-interface and the formation of complexes with functional binding sites at the mineral surface. Surface reactions are postulated and the related mass action and mass balance relations are used to simulate sorption at the mineral surface as a function of system chemistry. SCMs account for the pH dependence of surface charge development at the mineral-water interface through the use of electrostatic terms. Of the different SCMs, the Diffuse-Layer Model (DLM) is perhaps the simplest, using a two-layer representation of the mineral-water interface (Dzombak and Morel, 1990). In contrast to more complex multilayer models, the DLM assumes that supporting electrolytes such as Na^+ and Cl^- do not interact with the surface, and does not specifically address the effects of ionic strength on sorption except through the charge-potential relationship (Davis and Kent, 1990; Dzombak and Morel, 1990).

The sorption of actinides on a variably charged surface sorption site can be represented as a function of pH in a generalized surface reaction demonstrated here with Np(V):

$$> XOH^{o} + pNpO_2^{+} + nH_2O \hat{U} [> XOH_q - (NpO_2)_p (OH)_n]^{p+q-n-1} + (1+n-q)H^{+} \qquad [2]$$

where q is the protonation state of the sorption site (q = 0, 1, or 2 for deprotonated, neutral, and protonated, respectively), and p and n are the reaction coefficients for NpO_2^+ and H_2O. NpO_2^+ represents the aqueous Np(V) species and $[>XOH_q\text{-}(NpO_2)_p(OH)_n]^{p+q-n-1}$ represents the Np(V) surface complex. In the SCM approach, a coulombic correction is incorporated into the mass action expressions for surface reactions to extract the intrinsic equilibrium constants. Similar reactions can be written for other actinides such as uranium and plutonium.

In a general sense, the observed dependence of actinide sorption on pH and PCO_2 is a consequence of mass action effects and equilibrium chemistry in the surface reaction represented by Eq. (2). An increase in the activity of NpO_2^+ drives the equilibrium reaction forward towards increasing sorption. Complexing ligands such as dissolved carbonate in a CO_2 atmosphere tend to form aqueous actinide-carbonate complexes in competition with the sorbing surface. Carbonate competition for the available actinide increases with increasing pH, reducing the aqueous actinide activity and driving the reaction in Eq. (2) to the left (decreasing sorption). This explanation is, of course, simplistic due to the

synergistic effects between solution chemistry, sorption site protonation state, and speciation of the aqueous and surface actinide complexes.

Sorption Modeling—Diffuse-Layer Model Parameters

Several computer codes exist with the capability of modeling pH-dependent actinide sorption (PHREEQC, HYDRAQL, MINTEQA2) (Parkhurst and Appelo, 1999; Papelis et al., 1988; Allison et al., 1991). Applying geochemical models to radionuclide sorption requires thermodynamic data for the aqueous speciation of the radionuclide of interest and SCM parameters consistent with these data. The database for the geochemical equilibrium speciation code MINTEQA2, Version 3.11 (Allison et al., 1991) has been modified to include aqueous thermodynamic data for a number of radioelements important to HLW management (Turner et al., 1993). Postulated sorption reactions and DLM parameters (Table 1) were derived in previous reports (Pabalan et al., 1998; Turner, 1995; Turner et al., 1993, 1998) by interpreting available actinide sorption data using a simplified uniform DLM approach (Turner, 1995).

For the purposes of this study, five actinide elements are considered: Am(III), Np(V), Pu(V), Th(IV), and U(VI). All five of these radionuclides are an important part of the radionuclide inventory intended for Yucca Mountain (Kerrisk, 1985; Oversby, 1987). With the exception of Pu, all are considered to be predominantly in a single oxidation state in the oxidizing groundwaters assumed for Yucca Mountain. Pu may also be present in the +4 and +6 oxidation states, but only Pu(V) is considered here.

The DLM has specific limitations that may affect its applicability over a broad range of conditions or mineralogy, and the extent of chemical and physical conditions over which the model can be applied should be carefully considered. The DLM parameters (i.e., binding constant and surface reactions modeled) are based on a limited number of sorption experiments conducted over a limited range of PCO_2, M/V, and actinide concentrations (Pabalan et al., 1998; Turner, 1995; Turner et al., 1993, 1998). For simplicity, ion exchange reactions were not included in the model and only surface complexation was considered. Also, it is important to note that, although full aqueous speciation is incorporated in the model, the only surface reactions considered are protonation/deprotonation of surface sites and actinide sorption reactions. Calculated changes in sorption behavior are therefore limited to those resulting from changes in aqueous speciation of the radionuclide due to complexing with ligands in the groundwater. Direct competition for available surface sites with other radioelements or major and minor groundwater constituents is neglected. This may have an impact on how the effects of carbonate on sorption are considered in the model. If carbonate complexation of a given actinide (e.g., Th) is either considered to be small or neglected in the thermodynamic database, then carbonate will have only a small or negligible effect on sorption behavior.

PRELIMINARY APPROACHES FOR ADDRESSING CHEMICAL EFFECTS IN PERFORMANCE ASSESSMENT TRANSPORT/SORPTION MODELS

Computational requirements limit direct incorporation of geochemical sorption models into current PA codes, and it is likely that the use of PDFs for K_ds will continue in the next generation of PA codes. One approach to incorporating detailed model results in PA is to use them "off-line" to provide constraints on parameter uncertainty and account for site-specific geochemical variability. Two approaches are

described in this report and demonstrated using DLM sorption modeling with hydrochemical information specific to Yucca Mountain.

Estimating Sorption Parameter Probability Distribution Functions (PDFs)

One approach to accounting for geochemical effects on sorption behavior in PA is to develop the uncertainties represented by the K_d PDFs using process models to simulate sorption under observed variability in hydrochemistry in the vicinity of Yucca Mountain. A detailed description of the method as applied to Np(V) and U(VI) sorption is provided in Turner and Pabalan (1999). The approach has been extended to include Am(III), Th(IV), and Pu(V) DLM results. A summary is provided here.

Gathering Hydrochemical Data

Evaluating the effects of geochemistry on sorption at Yucca Mountain requires an understanding of the expected variability in key geochemical parameters. A convenient and comprehensive source of regional hydrochemistry data in the Yucca Mountain vicinity is the U.S. Geological Survey (USGS) report of Perfect et al. (1995) that compiles over 4,700 analyses from USGS reports and DOE reports and the USGS National Water Information Service (NWIS) database. Perfect et al. (1995) describes an editing philosophy to evaluate the raw data, remove duplicates, make chemical data entries consistent, and calculate charge balance. The editing philosophy is described in detail in the report.

It is assumed that the ranges of values of the chemical parameters reported in Perfect et al. (1995) represent the total variation that can be expected along potential flow paths in the Yucca Mountain hydrologic system during the 10,000 y postclosure period. The extent of the effects of the thermal loading of the repository is a design issue that is still under consideration by the DOE (Civilian Radioactive Waste Management System, Management and Operating Contractor, 2000b), and potential changes to the chemistry of the Yucca Mountain region due to the heat generated by the HLW are neglected. Perfect (1994) used cluster analysis to identify nine separate water chemistries related to lithology, but the sorption modeling approach described here was applied to the total range in hydrochemistry represented by all of the samples. Because of limitations in the source data, it is likely that the water chemistries reported for wells are from a mixture of several producing zones. Detailed sorption modeling using these data is assumed to represent the total range in a parameter such as K_d (or $K_{a'}$) due to geochemical effects.

To prepare the site-specific hydrochemistry for geochemical sorption modeling, Turner and Pabalan (1999) screened the data of Perfect et al. (1995) using geochemical criteria presented in Hitchon and Brulotte (1994). Uncertainties in sampling and measurement of key geochemical parameters such as pH suggested the need for additional examination of the data. For example, Hem (1985) noted that field pH measurements prior to the early 1950s are uncertain due to equipment or methodology. Turner and Pabalan (1999) therefore included an additional screening criterion limiting the dataset to post-1960 analyses on the assumption that more recent analyses are more traceable and reliable than older analyses. The final screening step was to limit the area covered to the vicinity of Yucca Mountain (Turner and Pabalan, 1999). The area (100 x 100 km) is much larger than the flow model used in typical PA calculations for Yucca Mountain (Civilian Radioactive Waste Management System, Management and Operating Contractor, 2000a; U.S. Nuclear Regulatory Commission 1999b,c), but it includes the most plausible flow paths to the location of likely receptor group(s) 10 to 30 km downgradient from

Yucca Mountain (Winograd and Thordarson, 1975) and to natural discharge and paleodischarge points to the southeast (Waddell, 1982; Paces et al., 1993). The final dataset contains 460 water analyses collected from 238 separate locations (Turner and Pabalan, 1999).

The database of water chemistries can be used to identify ranges and distribution types for key geochemical parameters in the ambient hydrochemical system at Yucca Mountain. For example, in the dataset, pH varied from 6.3 to 9.6 showing a normal distribution (or a lognormal distribution with respect to hydrogen activity). Inorganic carbon (C_T) showed a large range from 6.8 to greater than 10,000 $mg \cdot L^{-1}$ (Turner and Pabalan, 1999). The C_T data are skewed, however, by a small number (10 out of 460) brines collected from playas more than 50 km SW of Yucca Mountain that show a high C_T, and the bulk of the data are <1000 $mg \cdot L^{-1}$. The dataset also offers the opportunity to examine changes in hydrochemistry (and potentially radionuclide sorption) over a time period of several decades.

Because of a lack of vertical control on sampling intervals, local horizons of different chemistries may not be distinguishable. There is also a general lack of information on the redox condition of the water (e.g., Eh, dissolved O_2, pe, Fe^{3+}/Fe^{2+}), leaving a potentially critical parameter unconstrained. This uncertainty may be especially important for redox sensitive elements such as the actinides. The current approach used by both DOE and NRC in PA at Yucca Mountain assumes oxidizing conditions along the entire flow path (Civilian Radioactive Waste Management System, Management and Operating Contractor, 2000a; U.S. Nuclear Regulatory Commission, 1999b,c). This is considered to be conservative with regard to performance because most of the radionuclides (e.g., Np, U) are much more soluble and thought to be weaker sorbers under oxidizing conditions.

Using Yucca Mountain Hydrochemical Data in Sorption Modeling

For each of the 460 separate analyses, values of pH and the concentrations of the major species Ca^{2+}, Mg^{2+}, Na^+, K^+, HCO_3^-, CO_3^{2-}, SO_4^{2-}, Cl^-, F^-, Fe, and $SiO_2(aq)$ were written to an input file formatted for use with MINTEQA2, Version 3.11 (Allison et al., 1991). Temperature and pH were fixed at the measured values, Eh was unspecified due to a lack of measured data in the dataset, and measured Fe was assumed to be entirely Fe^{3+} (oxidizing conditions). Surface sorption reactions for the actinide-H_2O-CO_2-mineral system using the parameters listed in Table 1 were added to the major element hydrochemistry in the MINTEQA2 input file. Because of the lack of redox information, only a single oxidation state was modeled for each radionuclide.

The MINTEQA2 output was used to establish mean, minimum, and maximum values for sorption and transport parameter PDFs (Table 2). In the model results, a lognormal distribution seems to describe the calculated variability (Figure 8). Mean and median values are similar for each radioelement considered here (Table 2), suggesting that the distribution is not overly affected by extreme values. In addition to constraining PDFs for a given radioelement, this approach provides a means of developing a multivariate correlation among sorption parameter PDFs that reflects the underlying effects of geochemistry on sorption (Table 3). For example, calculating a distribution for Np(V) and U(VI) sorption can provide a bivariate correlation between Np(V) and U(VI) sorption that results from the effects of site-specific chemical variability. The correlation coefficient for Log K_d calculated for Np(V) and U(VI) is about 0.6, indicating a positive correlation in sorption behavior for these two actinides due to geochemical effects (Figure 9). The correlation is weak ($r^2 = 0.37$), however, due to the different speciation behavior of these two actinides, and is also likely influenced by a few outlier points. Correlation

coefficients calculated in a similar manner for multiple pairings of radioelements can be included as input into the PA sampling routine allowing the value selected for one radioelement sorption parameter to be conditioned by its geochemical relationship to the other radioelements. These types of correlations can also be used to examine the justification for using chemical analogues in PA to supplement limited sorption data for some radionuclides.

The spatial variability in hydrochemistry in the vicinity of Yucca Mountain is reflected in the large range in calculated sorption parameters (Table 2). One means of showing the variability in geochemical and sorption parameters is through the use of contour plots. Turner et al. (1999) created a geographic information system (GIS) coverage to show the spatial variation in potential radionuclide sorption that may have an effect on PA calculations (Figure 10). Calculated K_d for Np(V) is in the range of 25 to 100 $mL \cdot g^{-1}$ for most of the region downgradient from Yucca Mountain. In general, trends in potential sorption parallels trends in pH and PCO_2 along the axis of Amargosa Valley. Contour plots of a derived parameter such as K_d should be used carefully given the large number of groundwater properties that may potentially affect the model calculations. The map also shows that even with 238 separate sample locations, sampling density is concentrated in a few areas, and generally sparse over much of the region of interest. One way to address the sparse sample distribution is through the use of geostatistical techniques to show potential correlation lengths and directional anisotropy resulting from geochemical variability (Painter et al., 2001).

Performance Assessment Results and Sensitivity Analyses

The transport parameter PDFs and correlation coefficients developed using this approach were provided as input to the NRC TPA 3.1 code (U.S. Nuclear Regulatory Commission 1999b,c). Due to computational requirements, these correlations were only implemented for the Saturated Zone Alluvium unit (SAV) in the TPA input file. K_d values were converted to retardation factors (R_d) using the relationship:

$$R_d = 1 + \frac{\rho_b K_d}{\theta} \qquad [3]$$

where ρ_b is bulk density (g/cm^3) and θ is porosity (unitless). In calculating the R_d, ρ_b and θ are held constant at values used for alluvium in the TPA code. Only the sorption coefficient is treated as an uncertain parameter, so the variability of the retardation factor should reflect the variability in K_d. Sensitivity analyses are used to determine (i) whether the correlation coefficients were correctly implemented in TPA 3.1 sampling of the PDFs; (ii) the effects of correlated K_ds (or R_d) on dose as compared to the non-correlated K_ds of previous versions of the TPA code.

For the sensitivity analyses, total effective dose equivalent (TEDE) was calculated for individual radionuclides at 50,000 y for a critical group 20 km downgradient from the proposed repository. A total of 250 realizations were used to represent the range in TEDE resulting from parameter uncertainty.

Five transport parameters for the saturated alluvium were treated as variable, including R_d values for Am, Np, Pu, Th, and U. The PDFs for these R_d values were unchanged from the TPA 3.1 base case dataset, and runs were made either with or without correlation coefficients. All other parameters were

held at the base case values. An initial check of the K_d parameters sampled in the 250 realizations indicate that the TPA code is correctly including the correlation coefficients (Figure 11).

Preliminary sensitivity analyses results suggest that incorporation of correlation among K_ds does have an effect on predicted TEDE for these five radioelements relative to doses calculated assuming uncorrelated K_ds (Figure 12). As expected, the radionuclides most affected include those with correlations: ^{238}U, ^{237}Np, ^{230}Th, ^{241}Am. Other radionuclides (e.g., ^{226}Ra and ^{210}Pb) present in TPA 3.1 in the decay chain from $^{234}U \rightarrow {}^{230}Th \rightarrow {}^{226}Ra \rightarrow {}^{210}Pb$ also exhibit similar correlation effects on TEDE (Figure 12). The effect, however, does not appear to be systematic. For 250 realizations, calculated peak dose for all radionuclides assuming correlation among K_ds for can be either higher or lower than the uncorrelated case. Although individual realizations for a given radionuclide may be quite different, the predicted peak mean dose (all radionuclides) is essentially unchanged at 10,000 y (about 5 percent higher for the correlated case). The small effect is due in large part to the relatively robust waste packages predicted in the TPA 3.1 base case (U.S. Nuclear Regulatory Commission, 1999b,c), and the dominant contribution to dose of the high solubility, nonsorbing radionuclides ^{99}Tc and ^{129}I. Also, correlations are limited to a subset of the radionuclides tracked in TPA, and have only been considered for transport through the saturated alluvium. The expected dose curves for the correlated and uncorrelated case begin to diverge at longer times, after more waste packages have begun to fail and the contaminant plume reaches the saturated zone. The preliminary results suggest an additional level of uncertainty that should be considered in PA as correlations are developed for other radionuclides and implemented along the entire flow and transport pathway.

Sorption Response Surfaces

While using the DLM to constrain transport parameters PDFs is an approach that is quickly adapted to current PA approaches, it does not reduce the number of sampled parameters. Also, correlating among the different PDFs to reflect underlying geochemical effects on sorption is not efficient and brings a high computational burden to the PA calculations. Moreover, although the PDF method represents the variability of geochemical conditions, it does not represent the variation in a spatial sense. Site-specific values for geochemical and mineralogical properties could be used to better represent conditions along an expected flow path even if explicit geochemical coupling is not available in PA. This type of approach would use the DLM to generate a response surface that represented sorption as a function of several key parameters (e.g., pH and *P*CO2) (Figure 13). Using this method, measured site-specific values could be used in a more direct fashion. These parameters and their field-measured PDFs could be assigned to appropriate locations and stratigraphic horizons included in the PA model and sampled to determine the appropriate K_d values, based on SCM calculations, for the transport paths within each realization. While this is not an explicit incorporation of geochemistry in the transport calculations, it does provide a step toward a more sound theoretical basis for sorption modeling in PA. It also has the benefit of reducing the number of sampled parameters for each PA run.

Demonstrating the Response Surface for Np(V)

Since Np(V) sorption is known to be sensitive to a variety of system physicochemical conditions, several model simulations were conducted to assess the sensitivity of the model to system variables. DLM simulations were conducted using parameters in Table 1 over a range of pH, PCO_2, M/V, and Np(V)

concentration. The range in simulated conditions are summarized in Table 4. In general, for each model simulation, PCO_2 was held constant while pH was varied throughout a range from 2 to 11.75.

Following the simulations, the DLM-generated data were analyzed to identify important variables and evaluate significant trends and consistencies. Surface plots of results were generated. An effort was then made to evaluate the best approach to reproducing the sorption coefficient or response surface.

Sensitivity Analyses using Response Surfaces

Sensitivity of the Model to Variation in pH. Previous experimental results demonstrate that Np(V) sorption is sensitive to solution pH, and that Np(V) sorption follows a trend similar to the hydrolysis of the NpO_2^+ species in solution (Bertetti et al., 1996; 1998; Turner et al., 1998). The DLM reproduces the expected (Bertetti et al., 1998) pH dependency well (Figure 14). This behavior is consistent with that of other actinides (Allard et al., 1984; Hsi and Langmuir, 1985; McKinley et al., 1995; Turner et al., 1998).

Sensitivity of the Model to Variations in PCO_2. The PCO_2 in the model system also has a significant effect on the pH range and magnitude of Np(V) sorption (Figure 14). As PCO_2 increases, the pH at which Np(V) sorption reaches a maximum occurs at progressively lower pH values and the range of pH over which sorption is observed diminishes. The results are consistent with previous experimental results (Bertetti et al., 1998; Turner et al., 1998), but it is important to note that the model slightly underpredicts the magnitude of sorption at high pH values when CO_2 is present. This may be due to a lack of consideration of the sorption of Np-carbonate complexes or an overestimate of the presence of Np-carbonate complexes in solution. (Turner et al., 1998).

Sensitivity of the Model to Variation in M/V. As expected, the model is not particularly sensitive to variations in M/V (Figure 15). This occurs primarily because representation of results in terms of Kd , and subsequently $K_{a'}$, normalizes the data for differences in M/V. Additionally, for the low radionuclide concentrations expected, there is always an excess of available sorption sites, even at low M/V ratios. At very high M/V ratios, the high calculated surface areas effectively limit the sorption as represented by $K_{a'}$.

Sensitivity of the Model to Variation in Np(V) Concentration. The model results are not sensitive to variances in the Np(V) concentration, even over large range of concentrations examined (Figure 16). These results agree with experimentally derived results of Np(V) sorption (e.g., Girvin et al., 1991; Righetto et al., 1991; Bertetti et al., 1998).

These DLM sensitivity analyses suggest that actinide sorption is most sensitive to changes in pH and PCO_2. Therefore, pH and PCO_2 would be the most useful parameters to use in construction of a representative response surface for Np(V) sorption. Figure 17 is a three-dimensional response surface depicting the variation in $K_{a'}$ over a range of pH and PCO_2 (M/V and Np(V) concentration are held constant). The response surface represents values of $K_{a'}$, which are based on detailed DLM calculations, that can be quickly derived for use in PA using available site-specific geochemical parameters (i.e., pH and PCO2).

This approach carries a number of simplifying assumptions embedded in the detailed sorption model. Notwithstanding the limitations of the approach, the model has potential for application as part of the PA. There are several options for incorporating the sorption coefficient response surface. The

response surface or an interpolated version of the surface can be generated as a database or look-up table with indices of the appropriate geochemical parameters (e.g., pH and PCO_2). Alternatively, a mathematical representation of the response surface may be generated so that pH and PCO_2 could be entered into a function that would produce a sorption parameter output. Finally, a combination of the look-up table and mathematical representation of the DLM-generated response surface can be developed and applied using site-specific data.

Look-up Table or Interpolated Surface

The modeled Np(V) sorption surface shown in Figure 17 is a non-interpolated mesh consisting only of model generated data (mesh intersections). Representing the appropriate $K_{a'}$ for pH and PCO_2 values between the model points requires some form of interpolation. Use of computer-generated interpolated meshes to represent the data is often unsatisfactory, and specific interpolation between discrete points can be a computational burden. Interpolation may be, in part, avoided by producing a model data set on a finer scale (smaller grid size). Alternatively, input from site-specific data can be limited (through rounding, for instance) to values that correspond to the grid. In ether case, a look-up table in the form demonstrated by Table 5 (or some other matrix format suitable to PA) represents a simple and fast mechanism for extracting site-specific $K_{a'}$ values. Disadvantages include maintenance of a potentially large number of data tables for all radionuclides of interest and an additional level of uncertainty added in the interpolation.

Three-dimensional Mathematical Representation

A second approach to incorporating the $K_{a'}$ response surface in PA would be to represent the surface with an equation or set of equations. Mathematical descriptions of the response surface would have the advantage of representing a continuous range of values over the desired intervals of pH and PCO_2. Using the response surface shown in Figure 17, an attempt was made to fit a three-dimensional function to the surface using the 3-D curve fitting software (TableCurve 3-D, Jandel Scientific). Unfortunately, the resulting fits did not adequately reproduce the surface for the purposes of this study. Restricting the range of values considered did not result in an improved fit. Although, other response surfaces may be well represented mathematically, efforts to fit the Np(V) data were not continued.

Combination of Look-up and Mathematical Representation

A combination of mathematical modeling of the response surface and use of discrete look-up values may offer a reasonable solution for PA. Figure 18 shows the Np(V)-DLM results as a series of pH-dependent sorption curves for each PCO_2 modeled. Similarities in the shape of the sorption curves as a function of pH suggest that one equation form might be capable of fitting the curves. To test this, the pH-sorption curves were fit using TableCurve 2-D (Jandel Scientifc) to generate equations for the curves at each value of PCO_2. The range of data fit for each curve was limited to regions where sorption was predicted to be gretaer than zero. A relatively simple equation:

$$\ln(y) = a + bx + cx^2 + dx^3 + ex^4 + fx^5 \qquad [4]$$

(where a, b, c, d, and e are constants) adequately reproduces the model predicted sorption curves over the desired pH range for each value of PCO_2. Coefficients and goodness-of-fit values for each curve are

given in Table 6, and the fits are graphically represented in Figure 19. The fits are excellent, except for some deviations at low values of PCO_2, which are not reasonably expected in the field. The fitting exercise was limited to one equation form to simplify inclusion into PA. Alternative or multiple equations could be used to improve fits, but would add complexity to the modeling process. One advantage of this technique of incorporating the response surface is that only one parameter need be interpolated or restricted based on grid spacing to generate an appropriate sorption coefficient (K_d or $K_{a'}$). Since pH is typically measured with greater certainty than PCO_2, PCO_2 was selected to be the interpolated parameter. Similar response surfaces can be developed for other radionuclides (Figure 20).

A sample flow chart is presented using the combination look-up table and mathematical representation of the response surface (Figure 21). Required data for the sorption module include solution pH, PCO_2 (or equivalent), and mineral surface area. The chart shows those areas where additional modeling detail may be included (e.g., ion exchange) and where conservative assumptions of no sorption ($K_d = 0$) can be used. The proposed approach is flexible enough to be used with other modeling approaches and not limited to the DLM demonstrated here. Because the modeling is done off-line, additional detail (e.g., ion exchange) can be included without affecting the PA computation time.

Sampling Key Geochemical Parameters

Using K_d response surfaces in PA requires some means of sampling key geochemical parameters such as pH and C_T (or log PCO_2) and associating them with proper hydrostratigraphic units and spatial distributions. In the vicinity of Yucca Mountain, water chemistry databases such as those of Perfect et al. (1995) for saturated zone waters and Yang et al. (1996; 1998) for unsaturated zone waters provide a source of information for establishing PDFs for these parameters. Because of the link through carbonate aqueous chemistry, log PCO_2 and pH would be expected to be correlated; this information should be used in constraining sampling these geochemical parameters in PA. Other parameters like ionic strength or Na/Ca ratios might be more appropriate as sampled parameters for response surfaces developed using other modeling approaches, such as ion exchange. If data are available, the flow paths could be partitioned with respect to geochemical parameters. This type of refinement may be unwarranted for PA, however, given the uncertainty in changing geochemical conditions over the long times of interest and the sparseness of geochemical data for the flow and transport pathway.

Surface areas, which are required to convert response surface $K_{a'}$ values to K_ds, are theoretically measurable, but in practice are difficult to determine with certainty. One way to address this uncertainty is to develop S_a PDFs based on lab and field measurements. For example, Triay et al. (1997) report measured N_2-BET S_a values of 2.6 to 10 $m^2 \cdot g^{-1}$ for tuff samples from the vicinity of Yucca Mountain. A number of recent studies also develop theoretical relationships between reactive S_a and hydrologic parameters such as porosity, permeability, density, and pore radius (Arthur, 1996; Smith and Schafer, 1999). Appropriate values could then be associated with geologic and hydrologic unit models (Civilian Radioactive Waste Management System, Management and Operating Contractor, 2000d,e; U.S. Nuclear Regulatory Commission, 1999b,c) already used in PA.

DISCUSSION

Certain geochemical processes can both retard the transport of radionuclides, delaying arrival times at the critical group location(s), and reduce radionuclide concentrations at the point of exposure. An

understanding of geochemical processes that influence radionuclide transport may be used to compensate for uncertainties in hydrologic models of the Yucca Mountain system (Simmons et al., 1995).

Both of the SCM-based approaches applied here have several limitations. Models have been calibrated and tested against relatively small sorption datasets, particularly for Am(III), Th(IV), and Pu(V), and the models also focus on a surface complexation mechanism and neglect other potential mechanisms such as ion exchange. The DLM approach discussed here has many underlying simplifications including: (i) a constant site density (2.3 sites/nm^2), (ii) representation of sorption on aluminosilicate minerals by a combination of aluminol (>AlOH^0) and silanol (>SiOH^0) sites (Turner, 1995), and (iii) surface reactions that are postulated and used on the basis of the simplest reaction(s) to reproduce the observed data. Other potential difficulties are in the uncertainty in SCM electrostatic terms for natural materials and applying models based on single mineral experiments to complex natural mineral assemblages (Davis, 2001). For example, Davis et al. (1998) have developed a non-electrostatic sorption model to address this uncertainty for uranium transport.

There also remains a considerable degree of uncertainty in the aqueous thermodynamic data for a number of radionuclides of interest in HLW management. The Nuclear Energy Agency (NEA) Thermodynamic Data Base Project has produced volumes on uranium (Wanner and Forrest, 1994), americium (Silva et al., 1995) and technetium (Rard et al., 1999). Additional volumes in neptunium and plutonium are not yet available. And even for those volumes published, a number of key minerals and species may not be well constrained. For example, the NEA database for uranium does not include data for many key uranium-silicate minerals such as uranophane, haiweeite, and soddyite, and the equilibrium constant for the neutral aqueous species $UO_2(OH)_2^0$ is only bounded at the upper limit.

Still, the simplified SCM approach used here with the DLM accurately reproduces experimental data over the ranges on which the model is based and appears to be applicable for more than one mineral type. Mineral surface or rock surface areas may be used to normalize sorption data and the similar nature of sorption behavior suggests that the model has the potential for applicability to a number of minerals, especially silicates. Comparisons to data from similar mineral types conducted over a broader range of conditions show the model is able to represent changes in sorption behavior owing to modifications in system chemistry (e.g., pH and PCO_2). The relative insensitivity to M/V and Np(V) concentration within the model suggests that a relatively limited number of variables need to be tracked in PA.

Ideally, mechanistic sorption models such as SCMs or ion exchange would be directly incorporated into PA calculations using reactive transport codes. While hydrogeochemical transport codes may be used to examine particular aspects of reactive transport, however, the additional computational burden that results from coupling equations for geochemistry and fluid flow may be excessive for PA. This is even more important for stochastic approaches that rely on sampling techniques and many realizations to generate CCDFs and population statistics. It may be possible to use detailed sorption models such as the DLM off-line to support K_d selection and assess the effect of critical parameters such as pH and PCO_2 for site-specific conditions.

One approach is to use existing site-specific information on the physical/chemical system at Yucca Mountain to constrain variability in sorption behavior. The compilation of Perfect et al. (1995) is assumed to represent likely variations in regional hydrochemistry in the vicinity of Yucca Mountain during the regulatory time period. A simplified DLM is used with this hydrochemistry data to provide realistic

constraints on the PDFs used in PA to describe radionuclide sorption. The model results suggest that lognormal distributions of actinide sorption coefficients are appropriate; the total ranges in calculated sorption parameters are as much as nine orders of magnitude due to changes in observed hydrochemistry alone, but much of the lower part of the range is skewed by a relatively small set of carbonate-rich groundwaters. The statistical relationship between the calculated K_d PDFs also provides a demonstration of calculating correlation coefficients among radioelement sorption parameters that can be used to indirectly include the effects of geochemistry in PA calculations.

An alternative method for using detailed sorption models is to apply the model over a wide range of geochemical conditions and develop a sorption response surface as a function of key parameters. Unlike K_d, which is a derived value, geochemical parameters are properties of the physical-chemical system that can either be measured or assigned bounding limits. The calculated sorbed and aqueous concentrations can be used to develop a range in K_d values predicted as a function of these variables. While this is not an explicit incorporation of geochemistry in the transport calculations, it does provide a step toward a more theoretical basis for sorption modeling in PA.

The approaches outlined here are not limited either to Yucca Mountain, or to a specific type of mechanistic geochemical sorption model. They do provide a means of incorporating aspects of detailed model results into current PA codes. Considerations for future work in the application of these approaches to PA should include (i) evaluation of available data to apply similar approaches for other radionuclides, (ii) application of single mineral sorption models to natural mineral assemblages, (iii) extension of modeling to incorporate more than one set of experiments for development of surface reactions and binding constants, (iv) evaluation of the utility of incorporating ion exchange module, as appropriate, and (v) development of experiments that would aid in model validation.

CITED REFERENCES

Allard, B., U. Olofsson, and B. Torstenfelt. 1984. Environmental actinide chemistry. Inorg. Chim. Acta 94:205–221.

Allison, J.D., D.S. Brown, and K.J. Novo-Gradac. 1991. MINTEQA2/PRODEFA2, a geochemical assessment model for environmental systems: Version 3.0 user's manual. EPA/600/3-91/021. Environmental Protection Agency, Athens, GA.

Arthur, R.C. 1996. SITE-94: Adaptation of mechanistic sorption models for performance assessment calculations. SKI Report 96:34. Swed. Nucl. Power Inspectorate, Stockholm.

Bertetti, F.P., R.T. Pabalan, D.R. Turner, and M.G. Almendarez. 1996. Neptunium(V) sorption behavior on clinoptilolite, quartz and montmorillonite. p. 631–638. *In* W.M. Murphy and D.A. Knecht (eds.) MRS Symposium Proceedings Volume 412: Scientific Basis for Nuclear Waste Management–XVII. Mat. Res. Soc., Pittsburgh.

Bertetti, F.P., R.T. Pabalan, and M.G. Almendarez. 1998. Studies of neptunium^{V} sorption on quartz, clinoptilolite, montmorillonite, and α-alumina. p. 131–148. *In* E.A. Jenne (ed.) Adsorption of metals by geomedia. Academic Press, New York.

Carlos, B.A., S.J. Chipera, and D.L. Bish. 1995. Distribution and chemistry of fracture-lining minerals at Yucca Mountain, Nevada. LA-12977-MS. Los Alamos National Laboratory, Los Alamos, NM.

Civilian Radioactive Waste Management System, Management and Operating Contractor. 1998. Total system performance assessment-viability assessment (TSPA-VA) analyses technical basis document. B00000000-01717-4301 REV 01. Civilian Radioactive Waste Management System, Management and Operating Contractor, Las Vegas.

Civilian Radioactive Waste Management System, Management and Operating Contractor. 2000a. Total system performance assessment for the site recommendation. TDF-WIS-PA-00001 REV 00. Civilian Radioactive Waste Management System, Management and Operating Contractor, Las Vegas.

Civilian Radioactive Waste Management System, Management and Operating Contractor. 2000b. Repository safety strategy: Plan to prepare the safety case to support yucca mountain site recommendation and licensing considerations. TDR-WIS-RL-000001 REV04 ICN01. Civilian Radioactive Waste Management System, Management and Operating Contractor, Las Vegas.

Civilian Radioactive Waste Management System, Management and Operating Contractor. 2000c. Unsaturated zone flow and transport model process model report. TDR-NBS-HS-000002 REV00 ICN02. Civilian Radioactive Waste Management System, Management and Operating Contractor, Las Vegas.

Civilian Radioactive Waste Management System, Management and Operating Contractor. 2000d. Hydrogeologic framework model for the saturated-zone site-scale flow and transport model. ANL–NBS–HS–000033. Revision 00. Civilian Radioactive Waste Management System, Management and Operating Contractor, Las Vegas.

Civilian Radioactive Waste Management System, Management and Operating Contractor. 2000e. Geologic framework model (GFM3.1). MDL–NBS–GS–000002. Revision 00. Civilian Radioactive Waste Management System, Management and Operating Contractor, Las Vegas.

Davis, J.A. 2001. Surface complexation modeling of uranium(VI) adsorption on natural mineral assemblages. NUREG/CR-6708. U.S. Nuclear Regulatory Commission, Washington, DC.

Davis, J.A., and D.B. Kent. 1990. Surface complexation modeling in aqueous geochemistry. p. 177–260. *In* M.F. Hochella, Jr. and A.F. White (eds) Reviews in Mineralogy: Volume 23. Mineral-Water Interface Geochemistry. Mineral. Soc. Am., Washington, DC.

Davis, J.A., J.A. Coston, D.B. Kent, and C.C. Fuller CC. 1998. Application of the surface complexation concept to complex mineral assemblages. Environ. Sci. Technol. 32:2820–2828.

Dzombak, D.A., and F.M.M. Morel. 1990. Surface complexation modeling: Hydrous ferric oxide. John Wiley and Sons, New York.

Environmental Protection Agency. 1999. 40 CFR Part 197: Environmental radiation protection standards for Yucca Mountain, Nevada; Proposed rule. Fed. Reg. 64:46,976–47,016.

Girvin, D.C., L.L. Ames, A.P. Schwab, and J.E. McGarrah. 1991. Neptunium adsorption on synthetic amorphous iron oxyhydroxide. J. Colloid Interface Sci. 141:67–78.

Hayes, K.F., G. Redden, W. Ela, and J.O. Leckie. 1991. Surface complexation models: An evaluation of model parameter estimation using FITEQL and oxide mineral titration data. J. Colloid Interface Sci. 142:448–469.

Hem, J.D. 1985. Study and Interpretation of the Chemical Characteristics of Natural Waters. U.S. Geol. Surv. Water Supply Pap. 2254. U.S. Geol. Surv., Washington, DC.

Hitchon, B. and M. Brulotte. 1994. Culling criteria for "standard" formation water analyses. Appl. Geochem. 9:637–645.

Hsi, C-K.D. and D. Langmuir. 1985. Adsorption of uranyl onto ferric oxyhydroxides: Application of the surface complexation site-binding model. Geochim. Cosmochim. Acta 49:1931–1941.

Kerrisk, J. F. 1985. An Assessment of the Important Radionuclides in Nuclear Waste. LA-10414-MS. Los Alamos National Laboratory, Los Alamos, NM.

LaFlamme B.D.,and J.W. Murray. 1987. Solid/solution interaction: The effect of carbonate alkalinity on adsorbed thorium. Geochim. Cosmochim. Acta 51:243–250.

McKinley J.P., J.M. Zachara, S.C. Smith, and G.D. Turner. 1995. The influence of hydrolysis and multiple site-binding reactions on adsorption of U(VI) to montmorillonite. Clays Clay Miner. 43:586–598.

National Research Council. 1999. Disposition of high-level radioactive waste through geological isolation: development, current status, and technical and policy challenges. National Academy Press, Washington, DC.

Nuclear Energy Agency. 1998. Update on waste management policies and programmes. Nuclear Waste Bulletin No. 13. Nuclear Energy Agency, Issy-les-Moulineaux, France.

Oversby, V.M. 1987. Important radionuclides in high level nuclear waste disposal: Determination using a comparison of the US EPA and NRC regulations. Nucl. Chem. Waste Management 7:149–161.

Pabalan, R.T., and D.R. Turner. 1997. Uranium(6+) sorption on montmorillonite: Experimental and surface complexation modeling study. Aqueous Geochem. 2:203–226.

Pabalan, R.T., J.D. Prikryl, P.M. Muller, and T.B. Dietrich. 1993. Experimental study of uranium(6+) sorption on the zeolite mineral clinoptilolite. p. 777–782. *In* C. Interrante and R. Pabalan (eds.) MRS Symposium Proceedings Volume 294: Scientific Basis for Nuclear Waste Management–XVI. Mat. Res. Soc., Pittsburgh.

Pabalan, R.T., D.R. Turner, F.P. Bertetti, and J.D. Prikryl. 1998. Uranium^{VI} sorption onto selected mineral surfaces. p. 199–130. *In* E.A. Jenne (ed.) Adsorption of metals by geomedia. Academic Press, New York.

Paces, J.B., E.M. Taylor, and C.A. Bush. 1993. Late Quaternary history and uranium isotopic compositions of ground water discharge deposits, Crater Flat, Nevada. p. 1,573–1,580. *In* Proceedings From the Fourth International Conference on High Level Radioactive Waste Management, Am. Nucl. Soc., La Grange Park, IL.

Painter, S., V. Cvetkovic, and D.R. Turner. 2001. Effect of heterogeneity on radionuclide retardation in the alluvial aquifer near Yucca Mountain, Nevada. Groundwater (in press).

Papelis, C., K.F. Hayes, and J.O. Leckie. 1988. HYDRAQL: A program for the computation of chemical equilibrium composition of aqueous batch systems including surface complexation modeling of ion adsorption at the oxide/solution interface. Tech. Report 306. Dept. Civ. Eng., Stanford Univ., Stanford, CA.

Parkhurst, D.L., and C.A.J. Appelo. 1999. User's guide to PHREEQC (Version 2)—A computer program for speciation, batch-reaction, one-dimensional transport, and inverse geochemical calculations. U.S. Geol. Surv. Water-Resources Investigations Report 99-4259. U.S. Geol. Surv., Denver.

Perfect, D.L. 1994. Creation and analysis of a hydrochemical data base for the Death Valley region, Nevada and California. M.S. thesis. Colorado School of Mines, Golden, CO.

Perfect, D.L., C.C. Faunt, W.C. Steinkampf, and A.K. Turner. 1995. Hydrochemical data base for the Death Valley region, Nevada and California. U.S. Geol. Surv. Open-File Report 94-305. U.S. Geol. Surv., Denver.

Rard, J.A., M.H. Rand, G. Anderegg, and H. Wanner. 1999. Chemical thermodynamics series, Volume 3: Chemical thermodynamics of technetium. Nucl. Energy Agency, Org. Econom. Coop. Develop. Elsevier, New York.

Righetto, L., G. Bidoglio, G. Azimonti, and I.R. Bellobono. 1991. Competitive actinide interactions in colloidal humic acid-mineral oxide systems. Environ. Sci. Technol. 25: 1,913–1,919.

Sanchez, A.L., J.W. Murray, and T.H. Sibley. 1985. The adsorption of plutonium IV and V on goethite. Geochim. Cosmochim. Acta 49:2,297–2,307.

Serne, R. J., R. C. Arthur, and K.M. Krupka. 1990. Review of geochemical processes and codes for assessment of radionuclide migration potential at commercial LLW sites. PNL-7285. Pacific Northwest Laboratories, Richland, WA.

Silva, R.J., G. Bidoglio, M.H. Rand, P.B. Robouch, H. Wanner, and I. Puigdomenich. 1995. Chemical thermodynamics series, Volume 2: Chemical thermodynamics of americium. Nucl. Energy Agency, Org. Econom. Coop. Develop. Elsevier, New York.

Simmons, A.M., S.T. Nelson, P.L. Cloke, T.R. Crump, C.J. Duffy, W.E. Glassley, Z.E. Peterman, M.D. Siegel, D. Stahl, W.C. Steinkampf, and B.E. Viani. 1995. The critical role of geochemistry in the program approach. Dep. Energy Letter Report. U.S. Dep. Energy, Washington, DC.

Smith, R.W., and A.L. Schafer. 1999. Effective reactive surface area: An isotropic property of physically and chemically heterogeneous porous media. p. 1,051–1,058. *In* J. Lee and D. Wronkiewicz (eds.) MRS Symposium Proceedings Volume 556: Scientific Basis for Nuclear Waste Management–XXII. Mat. Res. Soc., Pittsburgh.

Triay, I.R., A. Meijer, J.L. Conca, K.S. Kung, R.S. Rundberg, E.A. Strietelmeier, C.D. Tait, D.L. Clark, M.P. Neu, and D.E. Hobart. 1997. Summary and synthesis report on radionuclide retardation for the Yucca Mountain Site Characterization Project. Milestone 3784M. LA-13262-MS. Chemical Science and Technology Division, Los Alamos National Laboratory, Los Alamos, NM.

Turner, D.R. 1995. A uniform approach to surface complexation modeling of radionuclide sorption. CNWRA 95-001. Center Nucl. Waste Regulatory Analyses. San Antonio.

Turner, D.R., and S.A. Sassman. 1996. Approaches to sorption modeling for high-level waste performance assessment. J. Contam. Hydrol. 21:311–332.

Turner, D.R. and R.T. Pabalan. 1999. Abstraction of mechanistic sorption model results for performance assessment calculations at Yucca Mountain, Nevada. Waste Manage. 19:375–388.

Turner, D.R., T. Griffin, and T.B. Dietrich. 1993. Radionuclide sorption modeling using the MINTEQA2 speciation code. p. 783–789. *In* C. Interrante and R. Pabalan (eds.) MRS Symposium Proceedings Volume 294: Scientific Basis for Nuclear Waste Management–XVI. Mat. Res. Soc., Pittsburgh.
Turner, D.R., R.T. Pabalan, and F.P. Bertetti. 1998. Neptunium(V) sorption on montmorillonite: An experimental and surface complexation modeling study. Clays Clay Miner. 46:256–269.

Turner, D.R., R.T. Pabalan, J.D. Prikryl, and F.P. Bertetti. 1999. Radionuclide sorption at Yucca Mountain, Nevada - Demonstration of an alternative approach for performance assessment. p. 583–590. *In* J. Lee and D. Wronkiewicz (eds.) MRS Symposium Proceedings Volume 556: Scientific Basis for Nuclear Waste Management–XXII. Mat. Res. Soc., Pittsburgh.

Turner, G.D., J.M. Zachara, J.P. McKinley, and S.C. Smith. 1996. Surface-charge properties and UO_2^{2+} adsorption of a surface smectite. Geochim. Cosmochim. Acta 60:3,399–3,414.

U.S. Department of Energy. 1998. *Viability Assessment of a Repository at Yucca Mountain.* DOE/RW-0508. U.S. Department of Energy, Office of Civilian Radioactive Waste Management, Las Vegas.

U.S. Nuclear Regulatory Commission. 1999a. 10 CFR Part 19 et al.: Disposal of high-level radioactive wastes in a proposed geological repository at Yucca Mountain, Nevada; Proposed rule. Fed. Reg. 64:8,640–8,679.

U.S. Nuclear Regulatory Commission. 1999b. NRC sensitivity and uncertainty analyses for a proposed HLW repository at Yucca Mountain, Nevada, using TPA 3.1. Conceptual models and data. NUREG-1668, Vol. 1. U.S. Nuclear Regulatory Commission, Washington, DC.

U.S. Nuclear Regulatory Commission. 1999c. NRC sensitivity and uncertainty analyses for a proposed HLW repository at Yucca Mountain, Nevada, using TPA 3.1 Results and Conclusions. NUREG-1668, Vol. 2. U.S. Nuclear Regulatory Commission, Washington, DC.

Waddell, R.K. 1982. Two-dimensional, steady-state model of ground-water flow, Nevada Test Site and vicinity, Nevada–California. U.S. Geol. Surv. Water Resources Investigations Report 82–4085. U.S. Geol. Surv., Denver.

Wanner, H., and I. Forest. 1992. Chemical thermodynamics series, Volume 1: Chemical thermodynamics of uranium. Nuclear Energy Agency, Org. Econom. Coop. Develop. Elsevier, New York.

Wanner, H., Y. Albinsson, O. Karnl, E. Wieland, P. Wersin, and L. Charlet. 1994. The acid/base chemistry of montmorillonite. Radiochim. Acta 66/67:733–738.

Wescott, R.G., M.P. Lee, N.A. Eisenberg, and T.J. McCartin. 1995. NRC iterative performance assessment Phase 2: Development of capabilities for review of a performance assessment for a high-level waste repository. NUREG-1464. U.S. Nuclear Regulatory Commission, Washington, DC.

Wilson, M.L., J.H. Gauthier, R.W. Barnard, G.E. Barr, and H.A. Dockery, E. Dunn, R.R. Eaton, D.C. Guerin, N. Lu, M.J. Martinez, R. Nilson, C.A. Rautman, T.H. Robey, B. Ross, E.E. Ryder, A.R. Schenker, S.A. Shannon, L.H. Skinner, W.G. Halsey, J.D. Gansemer, L.C. Lewis, A.D. Lamont, I.R. Triay, A. Meijer, D.E. Morris. 1994. *Total-System Performance Assessment for Yucca Mountain—SNL Second Iteration (TSPA-1993).* Volume 2. SAND93–2675. Albuquerque, NM: Sandia National Laboratories.

Winograd, I.J., and W. Thordarson. 1975. Hydrogeologic and hydrochemical framework, south-central Great Basin, Nevada–California with special reference to the Nevada Test Site. U.S. Geol. Surv. Prof. Pap. 712-C. U.S. Geol. Surv., Washington, DC.

Yang, I.C., G.W. Rattray, P. Yu.. 1996. Interpretation of chemical and isotopic data from boreholes in the unsaturated zone at Yucca Mountain, Nevada. U.S. Geol. Surv. Water Resources Investigations Rep. 96-4058. U.S. Geol. Surv., Denver.

Yang, I.C., P, Yu, G.W. Rattray, J.S. Ferarese, J.N. Ryan, 1998. Hydrochemical investigations in characterizing the unsaturated zone at Yucca Mountain, Nevada. U.S. Geol. Surv. Water Resources Investigations Rep. 98-4132. U.S. Geol. Surv., Denver.

Yeh, G.T., and V.S. Tripathi. 1989. A critical evaluation of recent developments in hydrogeochemical transport models of reactive multichemical components. Water Resour. Res. 25:93–108.

Yeh, G.T., and V.S. Tripathi. 1991 A model for simulating transport of reactive multispecies components: Model development and demonstration. Water Resour. Res. 27:3,075–3,094.

Zachara, J.M., and J.P. McKinley. 1993. Influence of hydrolysis on the sorption of metal cations by smectites: Importance of edge coordination reactions. Aquatic Sci. 55:250–261.

Figure Captions

Figure 1 Location of the proposed repository at Yucca Mountain, NV. Groundwater sample locations and geographical features discussed in the text are identified. The flow regime outline is from the TPA 3.1 model (U.S. Nuclear Regulatory Commission 1999b).

Figure 2 The Total System Performance Assessment "pyramid" representing the technical basis for the abstraction process (from Civilian Radioactive Waste Management System, Management and Operating Contractor, 2000a).

Figure 3 Effects of pH on U(VI) sorption on different silicate and aluminosilicate minerals. Data from Zachara and McKinley (1993), McKinley et al. (1996), and Pabalan et al. (1998).

Figure 4 Effects of PCO_2 on U(VI) sorption on clinoptilolite (data from Pabalan et al., 1998).

Figure 5 Effects of M/V ratio on U(VI) sorption on montmorillonite expressed in terms of (a) percent U(VI) sorbed; (b) K_d ($mL \cdot g^{-1}$) (data from Pabalan et al., 1998).

Figure 6 Sorption of U(VI) on different silicate and aluminosilicate minerals expressed in terms of (a) K_d ($mL \cdot g^{-1}$); (b) K_a ($mL \cdot m^{-2}$) (data from Pabalan et al., 1998).

Figure 7 Sorption data from Figure 6 expressed in terms of $K_{a'} = K_d/S_{ea}$. See text for detailed discussion.

Figure 8 Calculated sorption parameter PDFs. DLM parameters are from Table 1 with hydrochemical data from Perfect et al. (1995). See text for detailed discussion.

Figure 9 Corresponding Np(V)- and U(VI)-montmorillonite sorption coefficients (K_d in $mL \cdot g^{-1}$) calculated with MINTEQA2 using DLM parameters given in Table 1. Solid line shows linear regression to the data with 95 percent prediction limits (dotted lines). Dashed line shows Log $K_{d,U(VI)}$ = Log $K_{d,Np(V)}$ for reference. Water chemistry based on 460 analyses developed from the data of Perfect et al. (1995).

Figure 10 Contour map of Np(V)-montmorillonite K_d ($mL \cdot g^{-1}$) calculated using the DLM with parameters from Table 1 and hydrochemistry from Perfect et al. (1995). Contour interval is 25 $mL \cdot g^{-1}$. Heavy outline shows the flow model from Yucca Mountain (white) used in NRC TPA calculations (U.S. Nuclear Regulatory Commission, 1999b,c).

Figure 11 Checking TPA 3.1 (U.S. Nuclear Regulatory Commission, 1999b,c) sampled radionuclide transport parameters for uranium and neptunium (250 realizations). (a) Sampling from uncorrelated transport parameters ($r^2 = 4.2 \times 10^{-6}$). (b) Sampling from correlated transport parameters [$r^2 = 0.372$ as compared to 0.37 calculated using DLM and the hydrochemical data of Perfect et al. (1995)].

Figure 12 TPA 3.1 calculated peak dose ($rem \cdot y^{-1}$) for specific radionuclides to critical group at 20 km. Comparison of results using uncorrelated and correlated alluvium sorption parameters for Am(III), Np(V), Pu(V), Th(IV), and U(VI). Lines represent regression to data for each nuclide, as indicated. Correlation coefficients listed in Table 3. All other parameters set at baseline values and PDFs (U.S. Nuclear Regulatory Commission, 1999b,c).

Figure 13 Schematic diagram showing steps to developing a response surface for radionuclide sorption. (a) Model calibration against experimental data; (b) Sorption variability as a function of pH and M/V; (c) Sorption variability as a function of pH and C_T.

Figure 14 DLM results of Np(V) sorption plotted over a range of PCO_2 and pH. $Np(V)_{total} \sim 1 \times 10^{-6}$ M, M/V = 4 $g \cdot L^{-1}$. DLM parameters are from Table 1.

Figure 15 DLM results for Np(V) sorption at various M/V values under atmospheric CO_2 ($PCO_2 = 10^{-3.5}$ atm). $Np(V)_{total} \sim 1 \times 10^{-6}$ M. DLM parameters are from Table 1.

Figure 16 DLM results for Np(V) sorption at various Np(V) concentrations under atmospheric CO_2 ($PCO_2 = 10^{-3.5}$ atm). M/V = 4 $g \cdot L^{-1}$. DLM parameters are from Table 1.

Figure 17 Response surface for Np(V) sorption calculated using the DLM. Data are plotted from 10^{-7} to 10^{-2} atm (CO_2-free results not shown for clarity). $Np(V)_{total} \sim 1 \times 10^{-6}$ M, M/V = 4 $g \cdot L^{-1}$. DLM parameters are from Table 1.

Figure 18 Plot of DLM predictions of Np(V) sorption at discrete PCO_2 values. $Np(V)_{total} \sim 1 \times 10^{-6}$ M, M/V = 4 $g \cdot L^{-1}$. DLM parameters are from Table 1.

Figure 19 Plots of polynomial fits to DLM K_as (points) for selected discrete values of PCO_2. Polynomial coefficients are given in Table 6. Values listed in the upper left-hand corner of each plot show PCO_2 in atm for the particular data set and fit. DLM parameters are from Table 1.

Figure 20 Plot of DLM predictions of important HLW radionuclides at discrete PCO_2 values. DLM parameters are from Table 1.

Figure 21 Flow diagram showing an approach that can be used to incorporate geochemical sorption models in PA.

Table 1. DLM model parameters used in this study.

Radioelement-Mineral	Surface Complex	Binding constant	Reference
Np(V)-montmorillonite	$>AlO^-$	-9.73	Turner et al. (1998)
	$>AlOH_2^+$	8.33	Turner et al. (1998)
	>SiO-	-7.20	Turner et al. (1998)
	$>AlO\text{-}NpO_2(OH)^-$	-13.79	Turner et al. (1998)
	$>SiOH\text{-}NpO_2^+$	4.05	Turner et al. (1998)
U(VI)-montmorillonite	$>AlO^-$	-9.73	Pabalan and Turner (1997)
	$>AlOH_2^+$	8.33	Pabalan and Turner (1997)
	>SiO-	-7.20	Pabalan and Turner (1997)
	$>AlO\text{-}UO_2^+$	2.70	Pabalan and Turner (1997)
	$>SiO\text{-}UO_2^+$	2.60	Pabalan and Turner (1997)
	$>AlO\text{-}(UO_2)_3(OH)_5^\circ$	-14.95	Pabalan and Turner (1997)
	$>SiO\text{-}(UO_2)_3(OH)_5^\circ$	-15.29	Pabalan and Turner (1997)
Am(III)-γ alumina	$>AlO^-$	-9.73	Turner and Sassman (1996)
	$>AlOH_2^+$	8.33	Turner and Sassman (1996)
	$>AlO\text{-}Am^{2+}$	4.66	This study [modified Turner(1995)]
Pu(V)-γ alumina	$>AlO^-$	-9.73	Turner and Sassman (1996)
	$>AlOH_2^+$	8.33	Turner and Sassman (1996)
	$>AlO\text{-}PuO_2^\circ$	-2.18	This study [modified Turner(1995)]
Th(IV)-γ alumina	$>AlO^-$	-9.73	Turner and Sassman (1996)
	$>AlOH_2^+$	8.33	Turner and Sassman (1996)
	$>AlO\text{-}Th^{3+}$	15.3	This study [modified Turner(1995)]

Table 2. Descriptive statistics for calculated sorption coefficient PDFs (expressed as log $K_{a'}$ in $mL \cdot m^{-2}$) using the DLM approach outlined in the text.

log $K_{a'}$ ($mL \cdot m^{-2}$)	*Am(III)*	*Np(V)*	*Pu(V)*	*Th(IV)*	*U(VI)*
Mean	6.549	0.742	2.707	4.248	-0.032
Median	6.539	0.773	2.715	4.330	0.002
Mode	6.337	0.738	2.650	4.439	-0.158
Standard Deviation	0.748	0.422	0.305	0.583	0.975
Kurtosis	1.924	26.576	5.055	34.228	12.928
Skewness	0.118	-3.556	-0.148	-4.414	-2.318
Range	5.958	5.140	2.974	7.715	9.407
Minimum	3.160	-3.264	0.906	-1.780	-6.837
Maximum	9.119	1.876	3.881	5.935	2.570
Count	460	460	460	460	460

Table 3. Correlation coefficients among log K_a ($mL \cdot m^{-2}$) values calculated using DLM parameters in Table 1 and hydrochemistry data from Perfect et al. (1995).

log K_a ($mL \cdot m^{-2}$)	Am(III)	Np(V)	Pu(V)	Th(IV)	U(VI)
Am(III)	1				
Np(V)	0.837	1			
Pu(V)	0.964	0.881	1		
Th(IV)	0.112	0.260	0.109	1	
U(VI)	0.346	0.610	0.489	0.165	1

Table 4. Summary of conditions modeled using the DLM approach described in the text.

Run	pH range	PCO_2 (atm)	$Np(V)_{total}$	M/V ($g \cdot L^{-1}$)
1	2 to 11.75 in 0.25 increments	no CO_2, 10^{-7} through 10^{-2} atm in $10^{0.5}$ atm increments	8.9×10^{-7} M	4
2	2 to 11.75 in 0.25 increments	no CO_2, 10^{-7} through 10^{-2} atm in $10^{0.5}$ atm increments	2.0×10^{-11} M	4
3	2 to 11.75 in 0.25 increments	no CO_2, 10^{-7} atm, $10^{-3.5}$ atm	8.9×10^{-7} M	40
4	2 to 11.75 in 0.25 increments	no CO_2, 10^{-7} atm, $10^{-3.5}$ atm	8.9×10^{-7} M	400
5	2 to 11.75 in 0.25 increments	no CO_2, 10^{-7} atm, $10^{-3.5}$ atm	8.9×10^{-7} M	2000
6	2 to 11.75 in 0.25 increments	no CO_2, 10^{-7} atm, $10^{-3.5}$ atm	1.0×10^{-14} M	4
7	2 to 11.75 in 0.25 increments	no CO_2, 10^{-7} atm, $10^{-3.5}$ atm	1.0×10^{-18} M	4

Table 5. Sample look-up table for Np(V) sorption response surface ($K_{a'}$ in $mL \cdot m^{-2}$). $Np(V)_{total} = 10^{-6}$ molal, M/V = 4 $g \cdot L^{-1}$.

pH	Log PCO_2 (atm)											
	no CO_2	-7.00	-6.50	-6.00	-5.50	-5.00	-4.50	-4.00	-3.50	-3.00	-2.50	-2.00
2.00	0.2341	0.2341	0.2341	0.2341	0.2341	0.2341	0.2341	0.2341	0.2341	0.2341	0.2341	0.2341
2.25	0.2079	0.2079	0.2079	0.2079	0.2079	0.2079	0.2079	0.2079	0.2079	0.2079	0.2079	0.2079
2.50	0.2079	0.2079	0.2079	0.2079	0.2079	0.2079	0.2079	0.2079	0.2079	0.2079	0.2079	0.2079
2.75	0.2079	0.2079	0.2079	0.2079	0.2079	0.2079	0.2079	0.2079	0.2079	0.2079	0.2079	0.2079
3.00	0.2079	0.2079	0.2079	0.2079	0.2079	0.2079	0.2079	0.2079	0.2079	0.2079	0.2079	0.2079
3.25	0.2079	0.2079	0.2079	0.2079	0.2079	0.2079	0.2079	0.2079	0.2079	0.2079	0.2079	0.2079
3.50	0.2079	0.2079	0.2079	0.2079	0.2079	0.2079	0.2079	0.2079	0.2079	0.2079	0.2079	0.2079
3.75	0.2341	0.2341	0.2341	0.2341	0.2341	0.2341	0.2341	0.2341	0.2341	0.2341	0.2341	0.2341
4.00	0.2341	0.2341	0.2341	0.2341	0.2341	0.2341	0.2341	0.2341	0.2341	0.2341	0.2341	0.2341
4.25	0.2341	0.2341	0.2341	0.2341	0.2341	0.2341	0.2341	0.2341	0.2341	0.2341	0.2341	0.2341
4.50	0.2603	0.2603	0.2603	0.2603	0.2603	0.2603	0.2603	0.2603	0.2603	0.2603	0.2603	0.2603
4.75	0.2867	0.2867	0.2867	0.2867	0.2867	0.2867	0.2867	0.2867	0.2867	0.2867	0.2867	0.2867
5.00	0.3130	0.3130	0.3130	0.3130	0.3130	0.3130	0.3130	0.3130	0.3130	0.3130	0.3130	0.3130
5.25	0.3660	0.3660	0.3660	0.3660	0.3660	0.3660	0.3660	0.3660	0.3660	0.3660	0.3660	0.3660
5.50	0.4457	0.4457	0.4457	0.4457	0.4457	0.4457	0.4457	0.4457	0.4457	0.4457	0.4457	0.4457
5.75	0.5529	0.5529	0.5529	0.5529	0.5529	0.5529	0.5529	0.5529	0.5529	0.5529	0.5529	0.5529
6.00	0.6880	0.6880	0.6880	0.6880	0.6880	0.6880	0.6880	0.6880	0.6880	0.6880	0.6880	0.6880
6.25	0.9071	0.9071	0.9071	0.9071	0.9071	0.9071	0.9071	0.9071	0.9071	0.9071	0.9071	0.9071
6.50	1.2144	1.2144	1.2144	1.2144	1.2144	1.2144	1.2144	1.2144	1.2144	1.2144	1.2144	1.1862
6.75	1.6451	1.6451	1.6451	1.6451	1.6451	1.6451	1.6451	1.6451	1.6451	1.6451	1.6451	1.6451
7.00	2.3022	2.3022	2.3022	2.3022	2.3022	2.3022	2.3022	2.3022	2.3022	2.2716	2.2716	2.2412
7.25	3.2507	3.2507	3.2507	3.2507	3.2507	3.2507	3.2180	3.2180	3.2180	3.2180	3.1530	2.9915
7.50	4.5839	4.5839	4.5839	4.5839	4.5839	4.5839	4.5839	4.5839	4.5482	4.4770	4.2305	3.6147
7.75	6.4836	6.4836	6.4836	6.4836	6.4836	6.4836	6.4836	6.4433	6.3229	6.0063	5.1299	3.4481
8.00	9.1026	9.1026	9.1026	9.1026	9.1026	9.0555	9.0084	8.8682	8.3635	7.1849	4.8363	2.2107
8.25	12.4660	12.4660	12.4660	12.4660	12.4093	12.3528	12.1286	11.4713	9.8251	6.6868	3.0559	0.7971
8.50	16.5473	16.5473	16.5473	16.5473	16.4088	16.1344	15.3324	13.1591	8.9616	4.1608	1.1019	0.1035
8.75	21.2582	21.2582	21.1725	21.0872	20.7488	19.6822	16.8977	11.5793	5.4292	1.5000	0.1556	0.0000
9.00	26.0843	25.9802	25.8765	25.4658	24.1749	20.8329	14.3720	6.8099	1.9102	0.2079	0.0000	0.0000
9.25	30.3776	30.1340	29.6530	28.2587	24.5651	17.1821	8.2733	2.3635	0.2867	0.0000	0.0000	0.0000
9.50	33.8870	33.0697	31.6281	27.8093	19.8431	9.7760	2.8637	0.3395	0.0258	0.0000	0.0000	0.0000
9.75	36.7831	34.5856	30.8712	22.6727	11.6335	3.4813	0.4457	0.0258	0.0000	0.0000	0.0000	0.0000
10.00	40.8242	35.3007	27.1492	14.7507	4.6556	0.6067	0.0258	0.0000	0.0000	0.0000	0.0000	0.0000

Table 6. Equation parameters and summary of fit results for model curves at discrete PCO_2. $Np(V)_{total} = 10^{-6}$ molal, M/V = 4 g·L^{-1}.

PCO_2 (atm)	Coefficients: [ln ($K_{g'}$, in mL·m^{-2}) = a + bx + cx^2 + dx^3 + ex^4 + fx^5]							
	a	b	c	d	e	f	r^2 value	pH range used for fit
$10^{-2.0}$	-323.7345	151.4137	-17.3990	-1.7541	0.4728	-0.0248	0.9999	6–9.25
$10^{-2.5}$	-441.4873	226.8171	-37.7489	1.2089	0.2378	-0.0167	0.9999	6–9.25
$10^{-3.0}$	148.2266	-173.8279	69.4791	-12.8694	1.1394	-0.0391	0.9999	6–9.50
$10^{-3.5}$	604.4445	-474.5178	147.2075	-22.6668	1.7365	-0.0529	0.9999	6–9.50
$10^{-4.0}$	847.1362	-620.1545	180.5362	-26.2031	1.8993	-0.0550	0.9999	6–10.00
$10^{-4.5}$	925.7299	-652.8079	183.1898	-25.6434	1.7940	-0.0502	0.9999	6–10.25
$10^{-5.0}$	923.2319	-632.0906	172.1421	-23.3804	1.5873	-0.0431	0.9999	6–10.50
$10^{-5.5}$	672.7843	-452.9837	121.1472	-16.1548	1.0778	-0.0288	0.9999	6–11.00
$10^{-6.0}$	393.8475	-258.6709	67.3401	-8.7496	0.5711	-0.0150	0.9999	6–11.25
$10^{-6.5}$	722.6946	-436.2311	104.2139	-12.3724	0.7340	-0.0175	0.9978	6–11.50
$10^{-7.0}$	2202.1902	-1290.5774	299.2739	-34.3782	1.9602	-0.0444	0.9816	6–11.75
no CO_2	1211.3978	-705.8275	161.4080	-18.1364	1.0037	-0.0219	0.9996	6–11.75

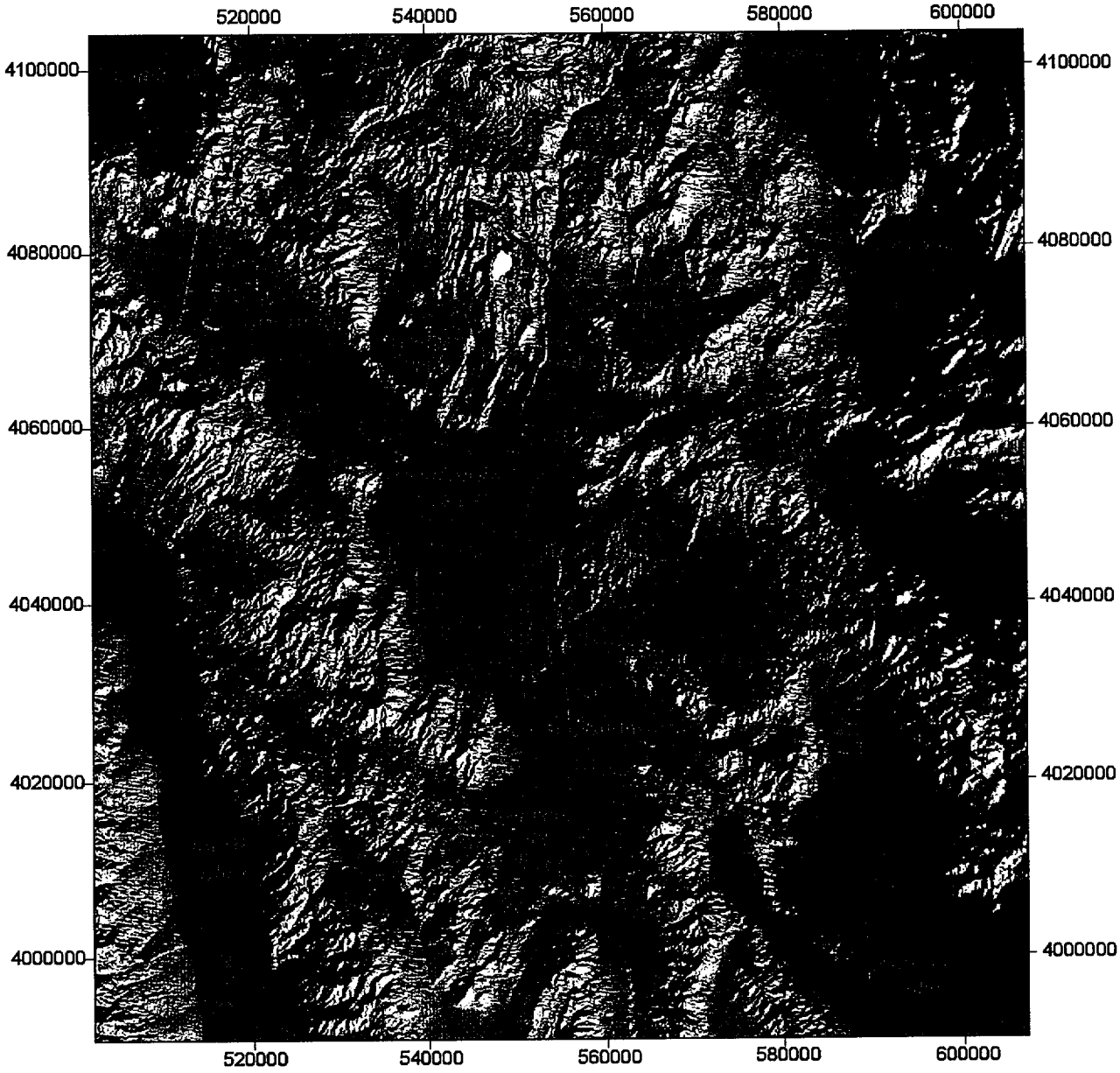
520000
540000
560000
580000
600000
4100000
4080000
4060000
4040000
4020000
4000000


NEVADA
Yucca Mountain
CALIFORNIA

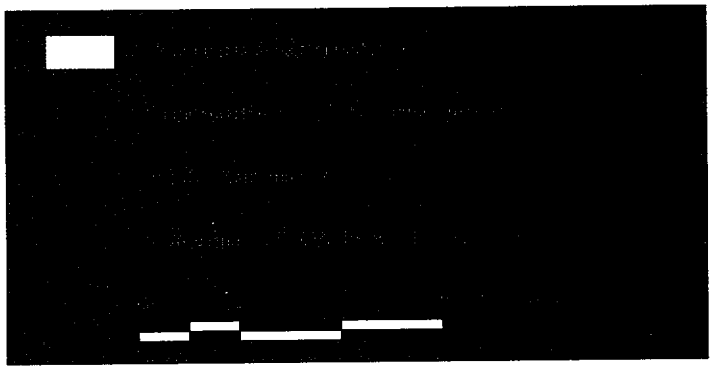

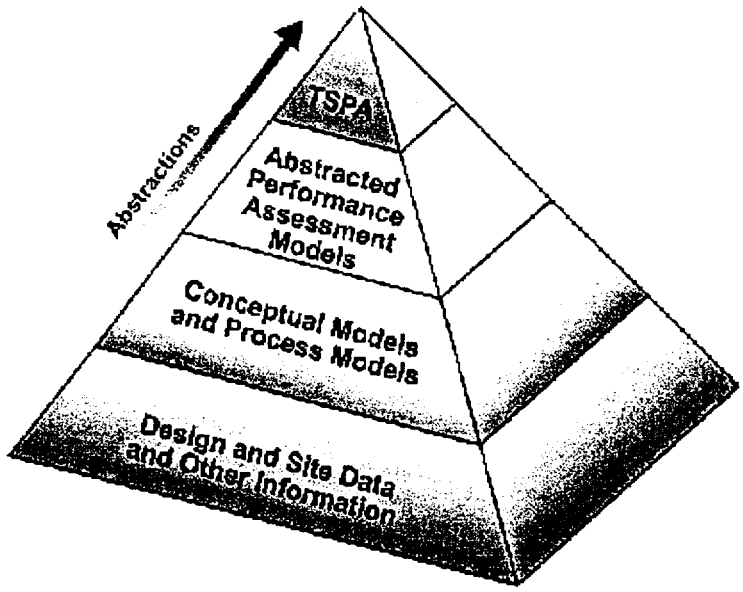
Abstractions
TSPA
Abstracted Performance Assessment Models
Conceptual Models and Process Models
Design and Site Data and Other Information

Figure 2

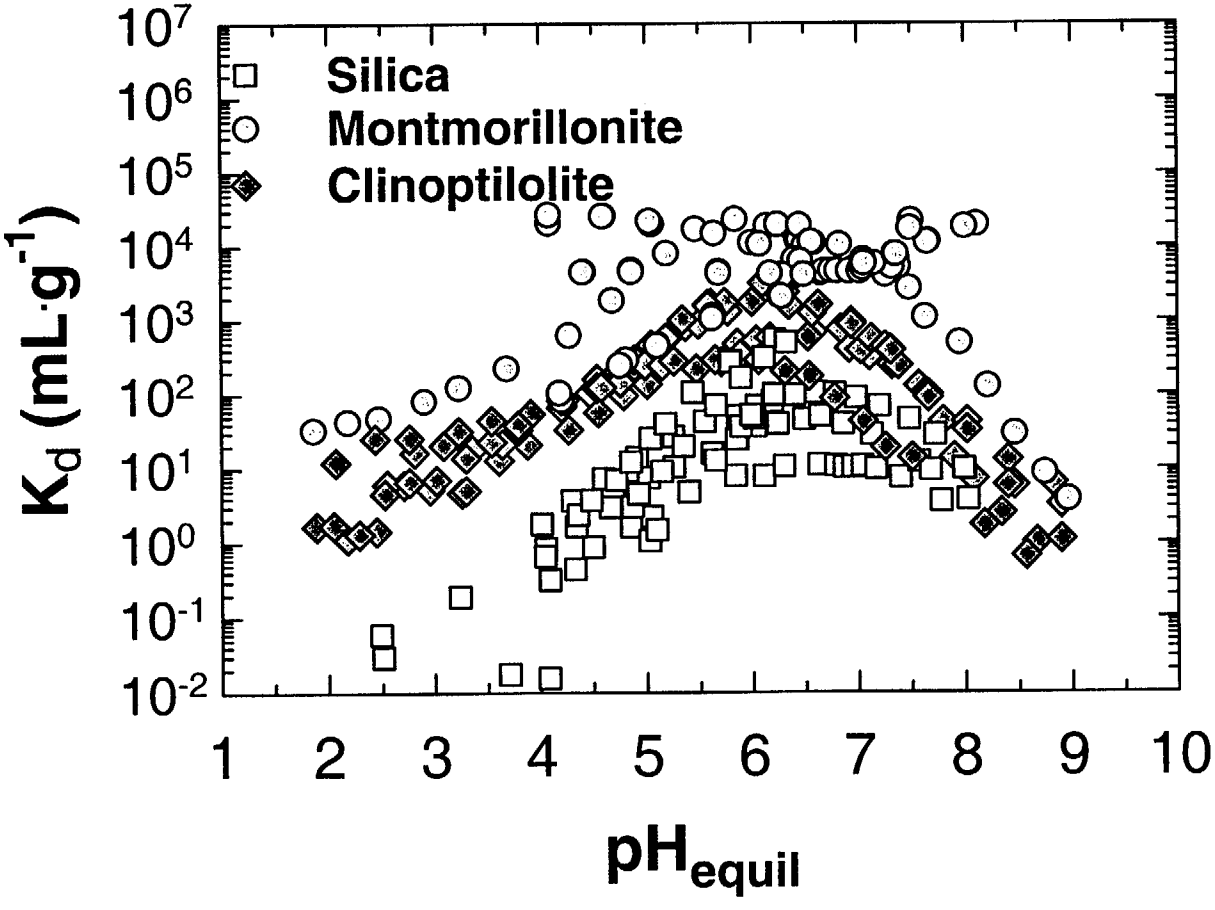
Silica
Montmorillonite
Clinoptilolite
K_d (mL·g^{-1})
10^7
10^6
10^5
10^4
10^3
10^2
10^1
10^0
10^{-1}
10^{-2}
1 2 3 4 5 6 7 8 9 10
pH_{equil}

Figure 3

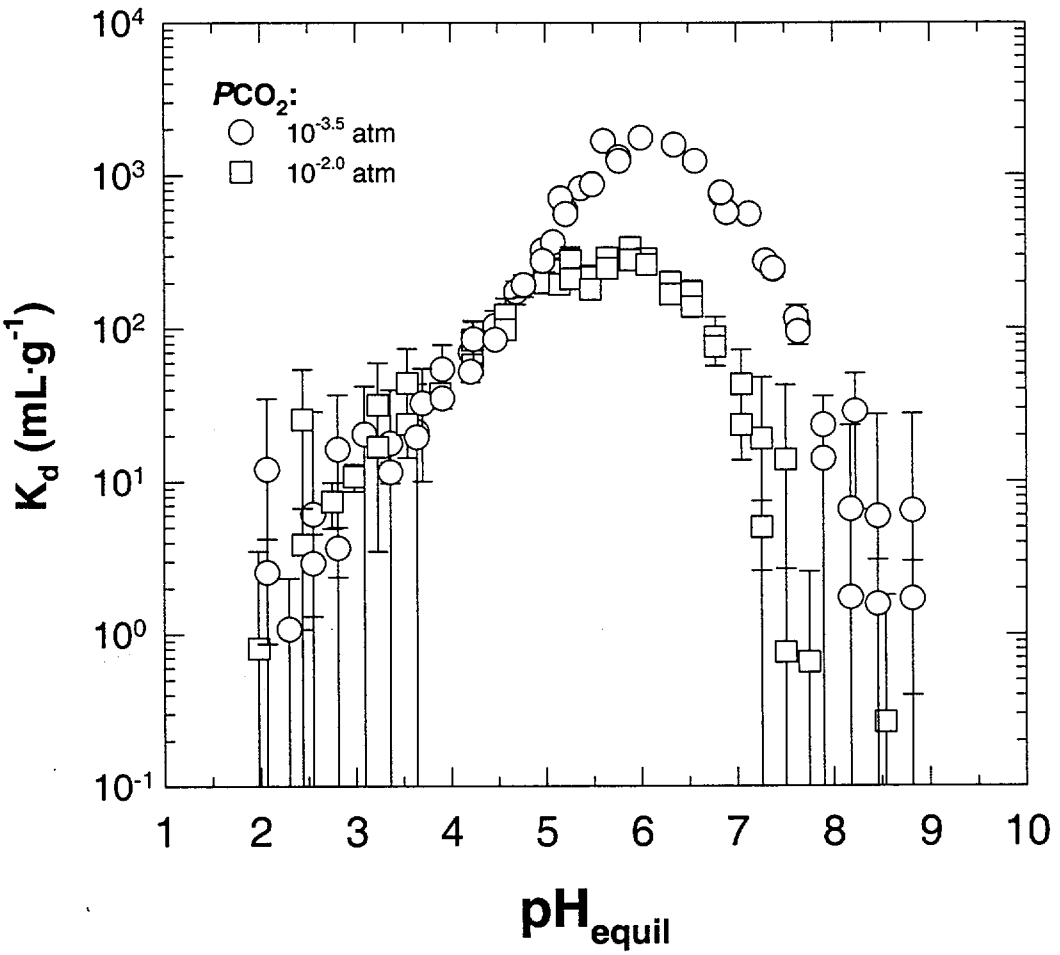
10^4
10^3
10^2
10^1
10^0
10^{-1}
K_d (mL·g^{-1})
PCO_2:
$10^{-3.5}$ atm
$10^{-2.0}$ atm
1
2
3
4
5
6
7
8
9
10
pH_{equil}

Figure 4

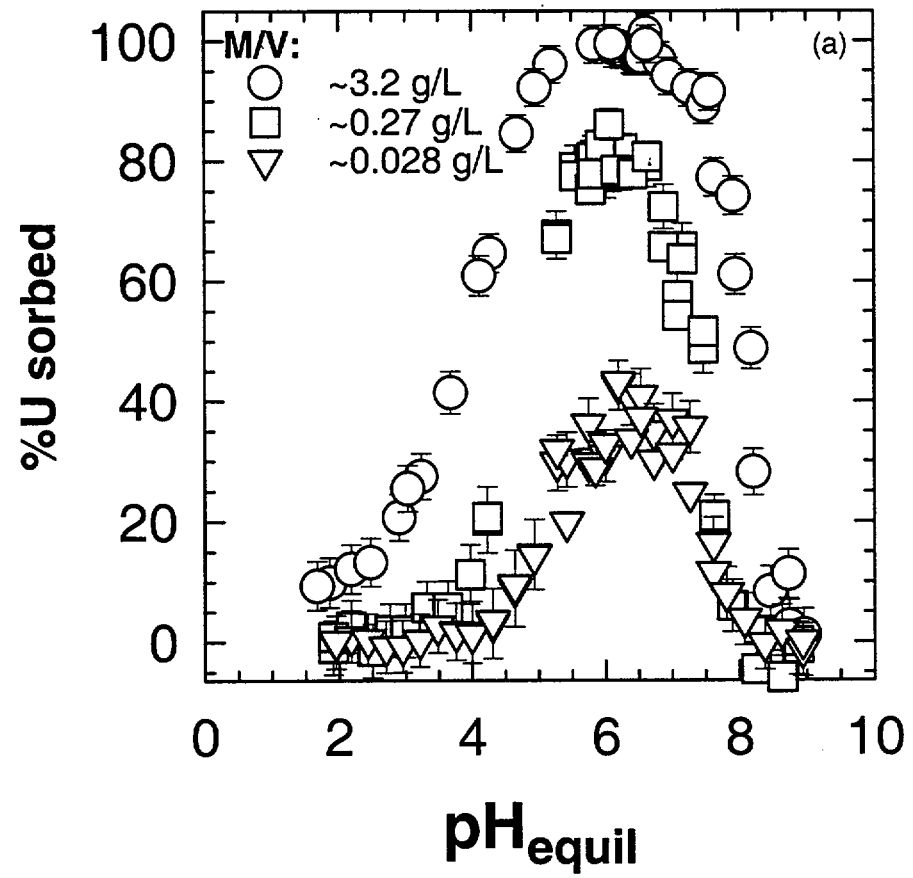
M/V:
~3.2 g/L
~0.27 g/L
~0.028 g/L
(a)
%U sorbed
pH equil

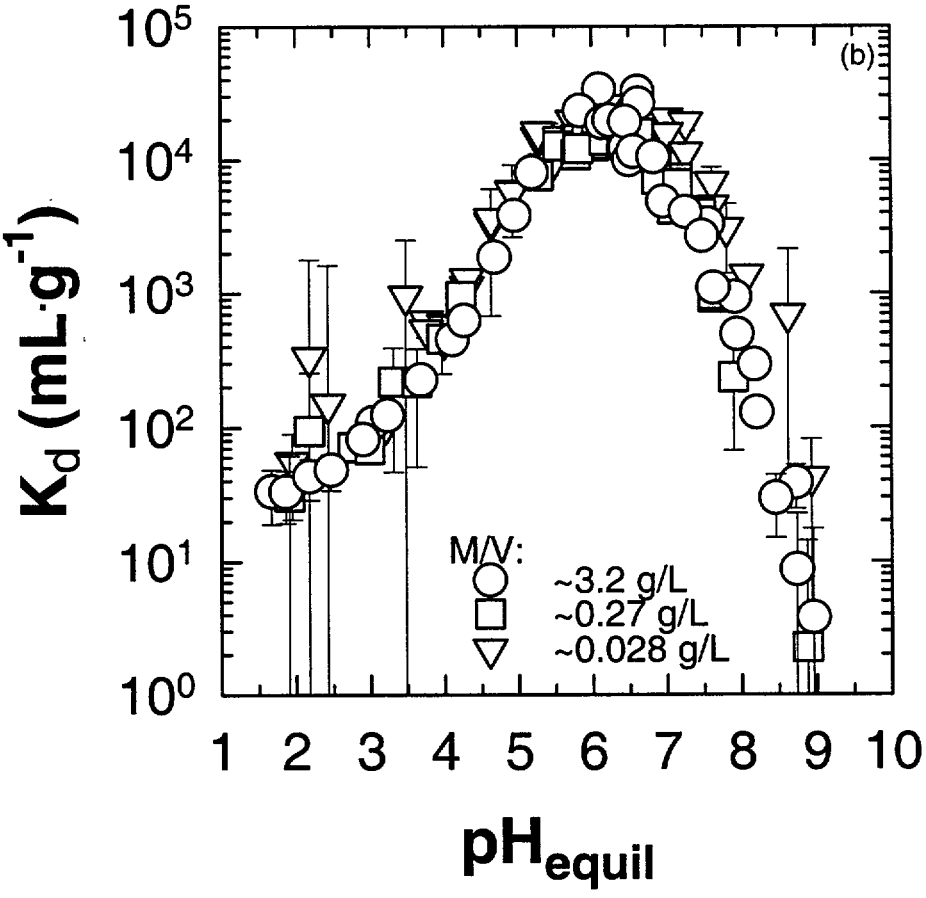
(b)
M/V:
~3.2 g/L
~0.27 g/L
~0.028 g/L
K d (mL·g-1)
pH equil

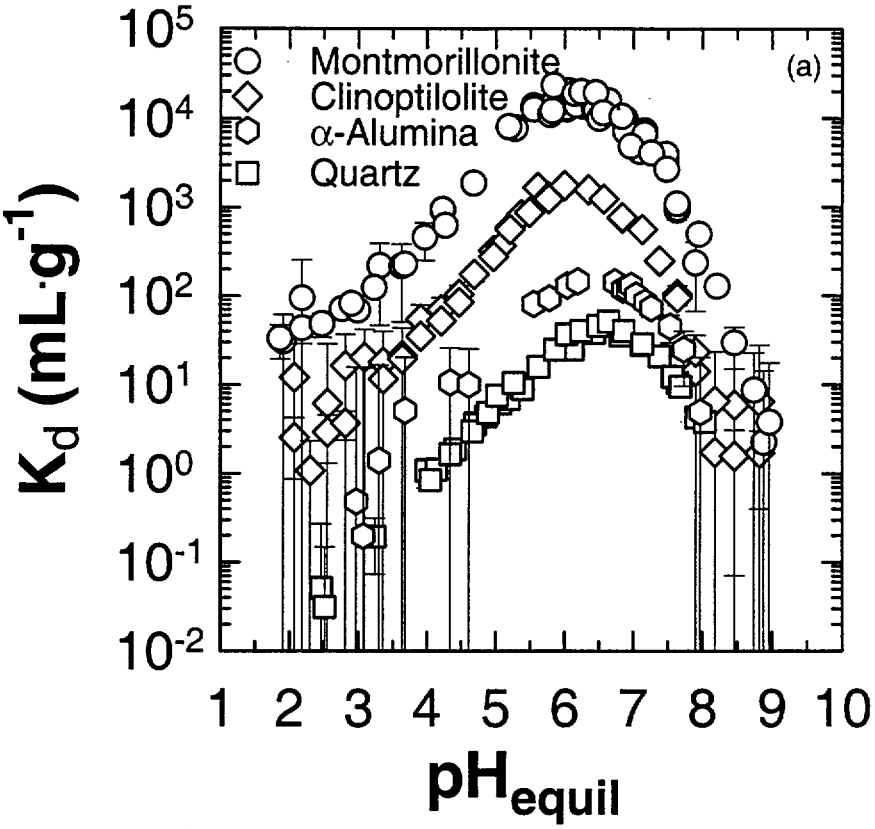
Montmorillonite
Clinoptilolite
α-Alumina
Quartz
(a)
K_d (mL·g^{-1})
10^5
10^4
10^3
10^2
10^1
10^0
10^{-1}
10^{-2}
1 2 3 4 5 6 7 8 9 10
pH_{equil}

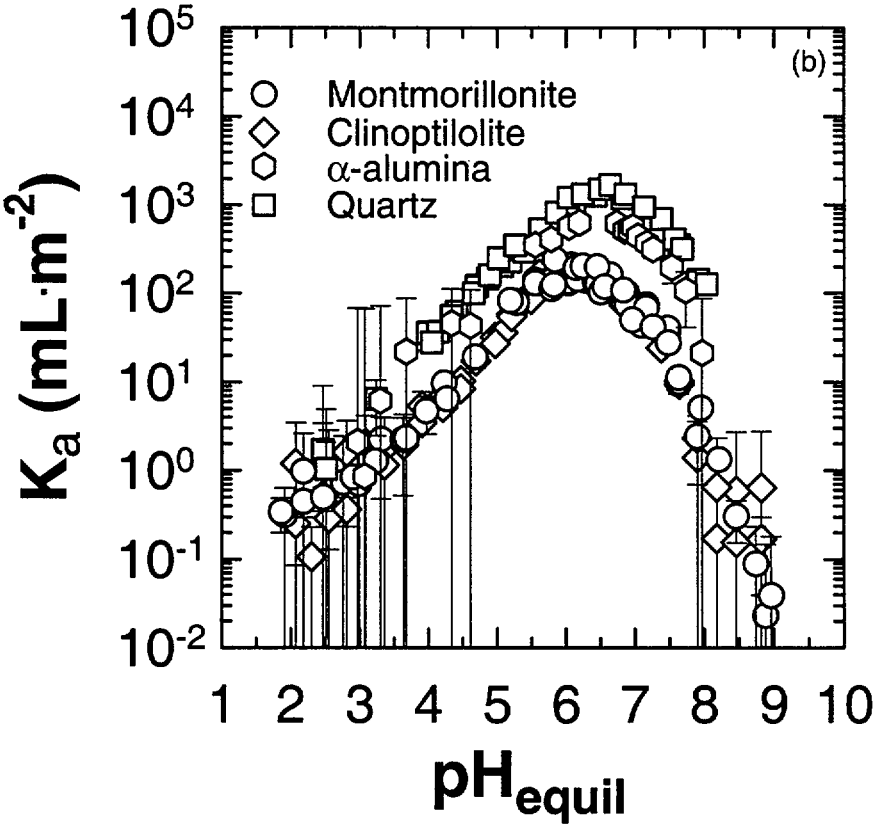
Montmorillonite
Clinoptilolite
α-alumina
Quartz
(b)
K_a (mL·m^{-2})
10^5
10^4
10^3
10^2
10^1
10^0
10^{-1}
10^{-2}
1 2 3 4 5 6 7 8 9 10
pH_{equil}

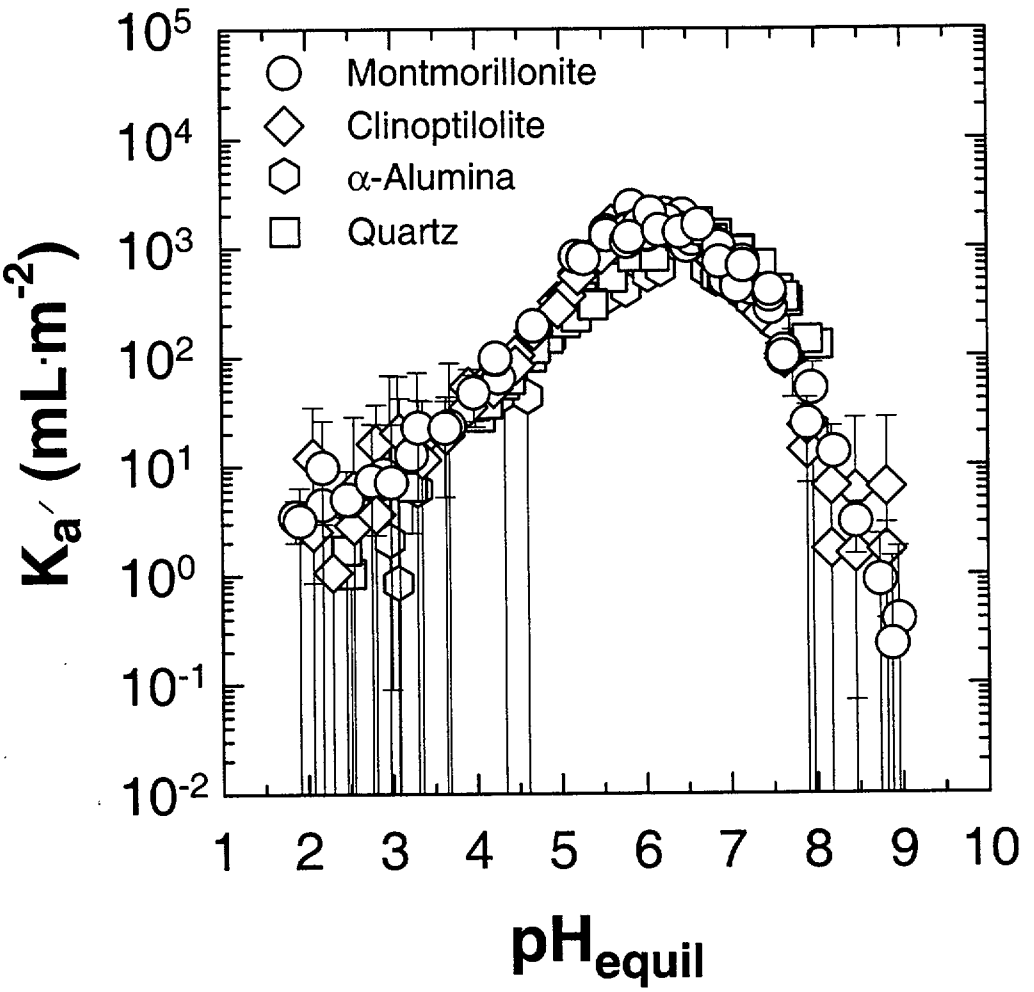
Montmorillonite
Clinoptilolite
α-Alumina
Quartz
K_a′ (mL·m^{-2})
10^5
10^4
10^3
10^2
10^1
10^0
10^{-1}
10^{-2}
1 2 3 4 5 6 7 8 9 10
pH_{equil}

Figure 7

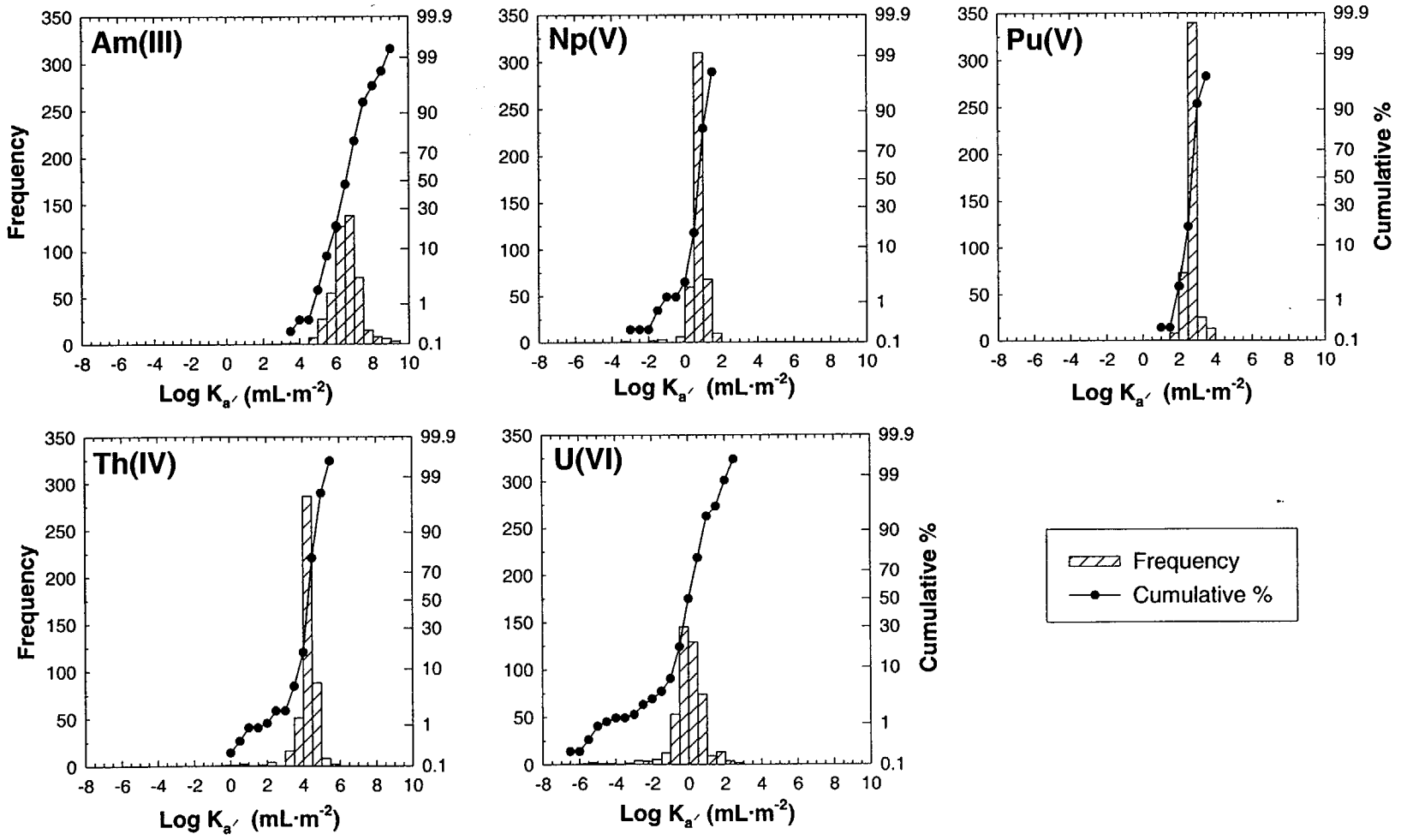
Am(III)
Np(V)
Pu(V)
Th(IV)
U(VI)
Frequency
Cumulative %
Log $K_{a'}$ (mL·m^{-2})
Frequency
Cumulative %

Figure 8

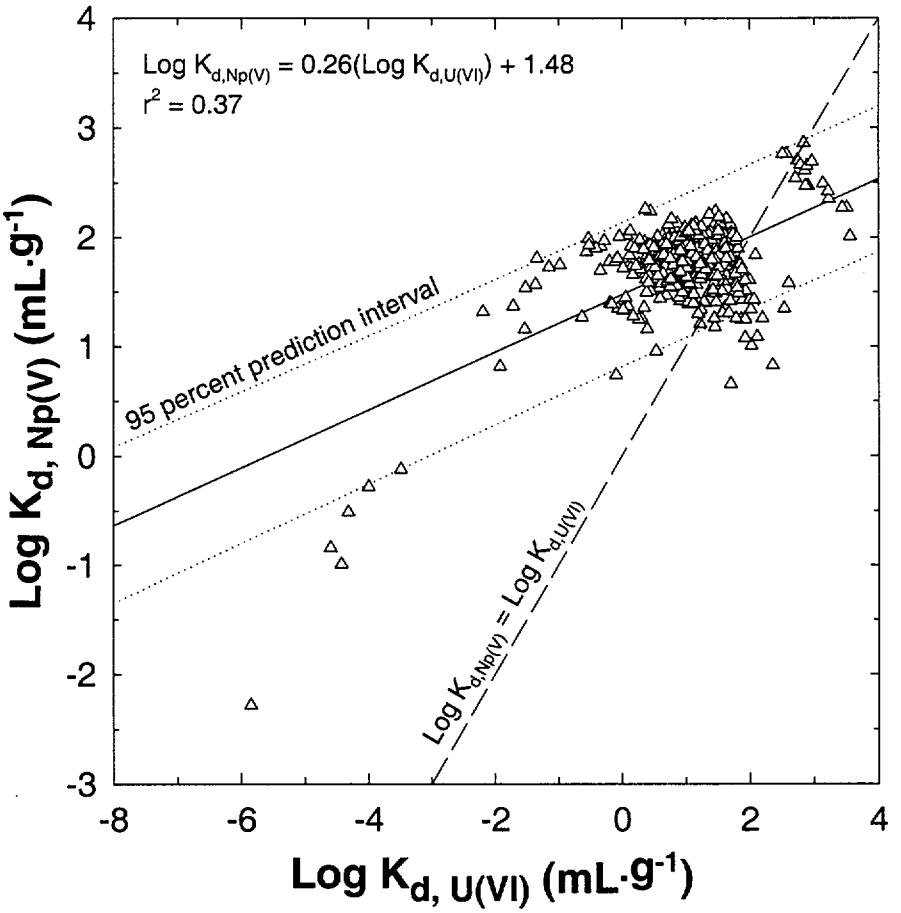
Log $K_{d,Np(V)}$ = 0.26(Log $K_{d,U(VI)}$) + 1.48
r^2 = 0.37
95 percent prediction interval
Log $K_{d,Np(V)}$ = Log $K_{d,U(VI)}$
Log $K_{d,\ Np(V)}$ ($mL \cdot g^{-1}$)
Log $K_{d,\ U(VI)}$ ($mL \cdot g^{-1}$)
4
3
2
1
0
-1
-2
-3
-8
-6
-4
-2
0
2
4

Figure 9

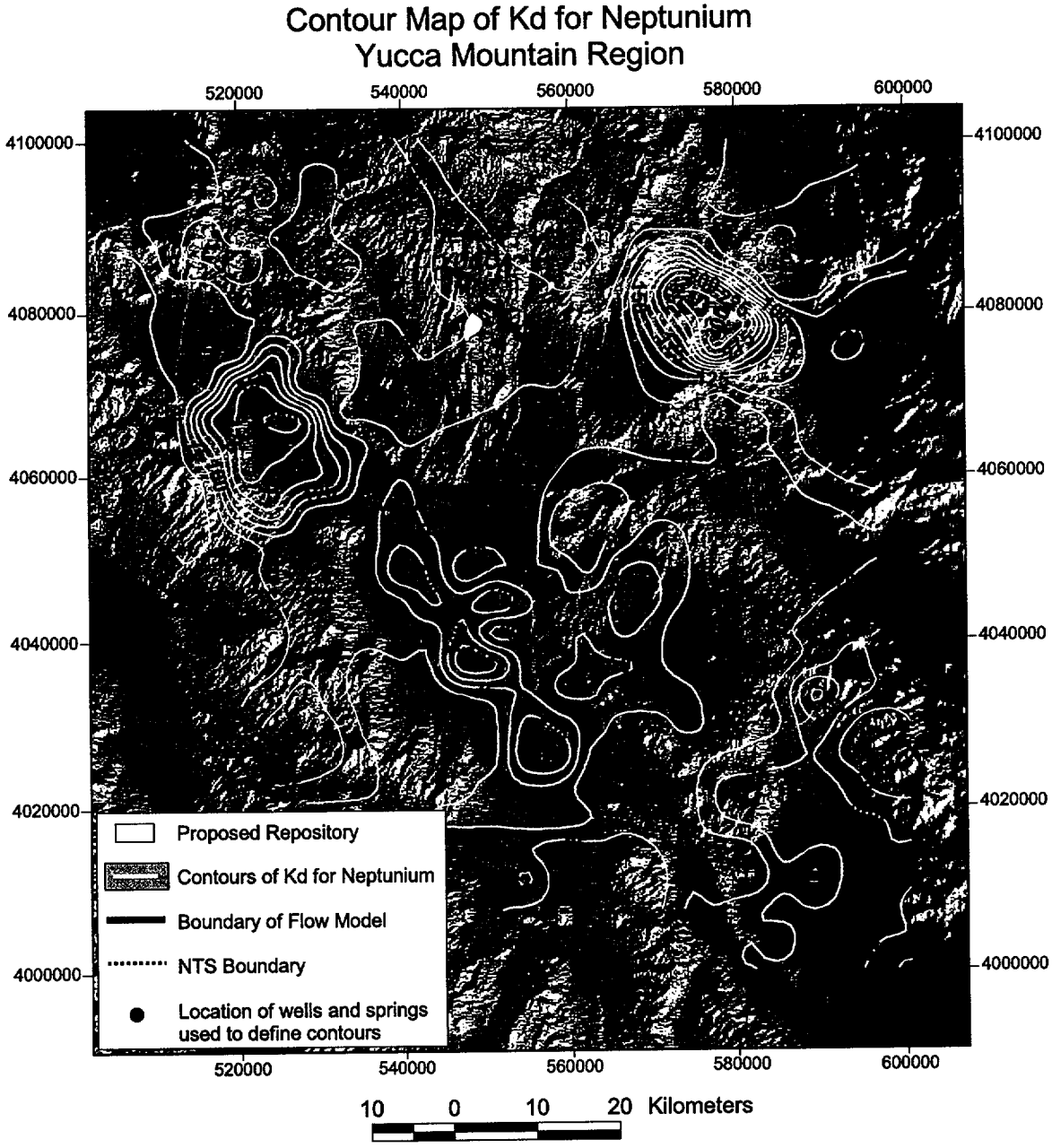
Contour Map of Kd for Neptunium
Yucca Mountain Region
520000
540000
560000
580000
600000
4100000
4080000
4060000
4040000
4020000
4000000
Proposed Repository
Contours of Kd for Neptunium
Boundary of Flow Model
NTS Boundary
Location of wells and springs used to define contours
10 0 10 20 Kilometers

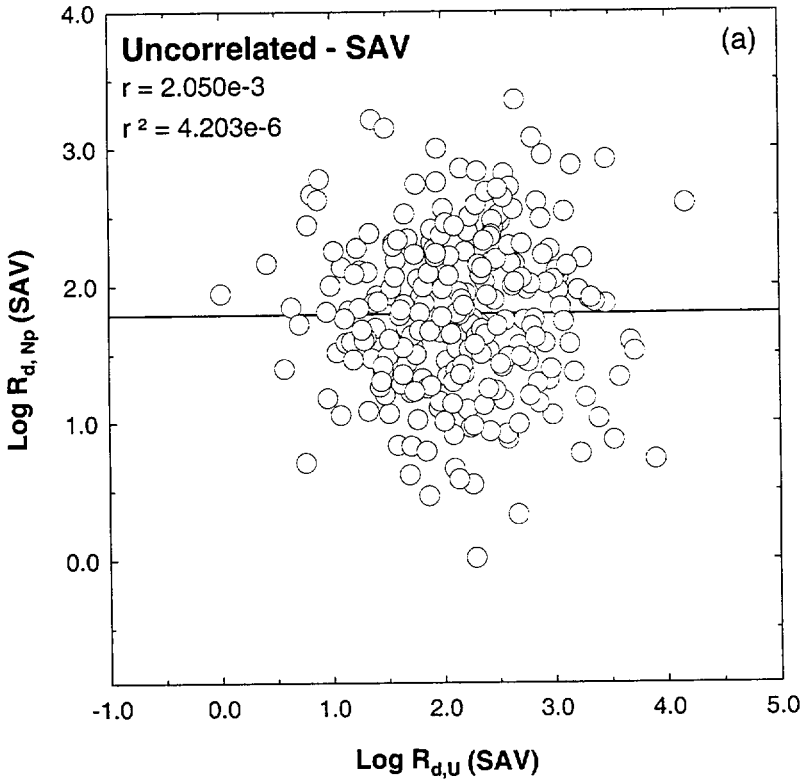
Uncorrelated - SAV
(a)
r = 2.050e-3
r ² = 4.203e-6
4.0
3.0
2.0
1.0
0.0
-1.0
0.0
1.0
2.0
3.0
4.0
5.0
Log R d, Np (SAV)
Log R d,U (SAV)

Fig. 11a

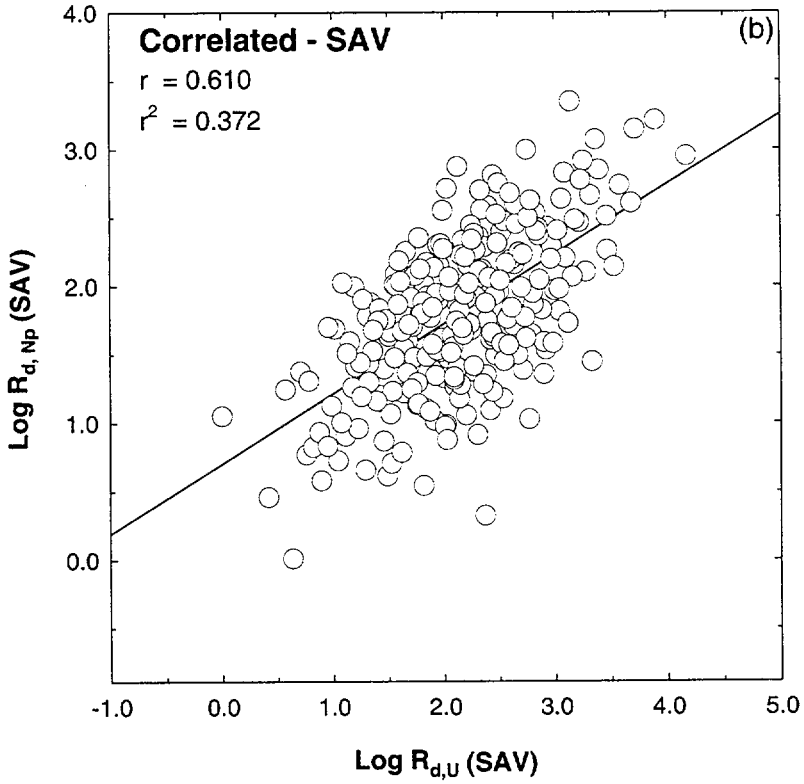
Correlated - SAV
r = 0.610
r² = 0.372
(b)
Log R_d, Np (SAV)
Log R_d,U (SAV)
4.0
3.0
2.0
1.0
0.0
-1.0
0.0
1.0
2.0
3.0
4.0
5.0

Figure 11b

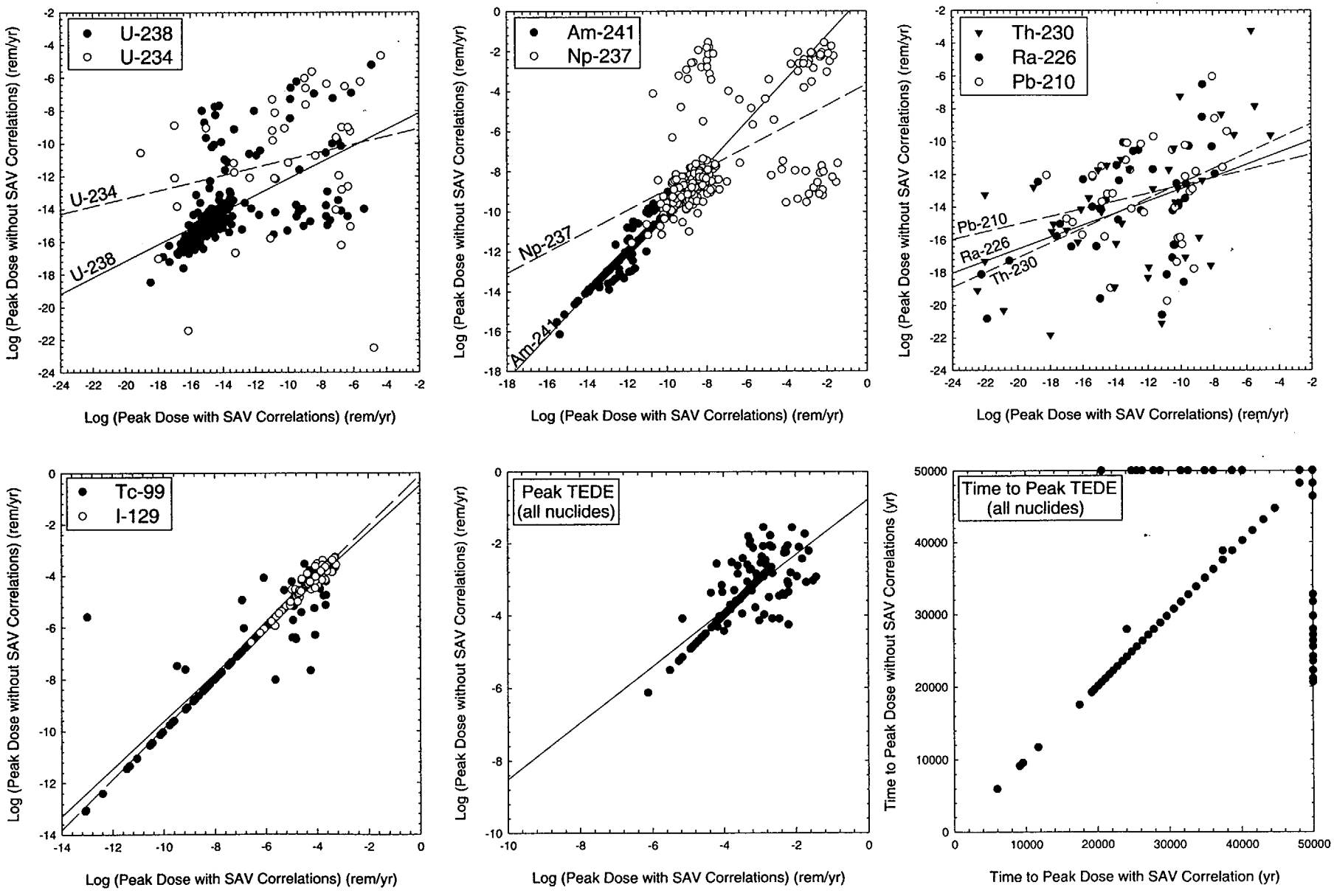
U-238
U-234
U-234
U-238
Log (Peak Dose without SAV Correlations) (rem/yr)
Log (Peak Dose with SAV Correlations) (rem/yr)
Am-241
Np-237
Np-237
Am-241
Log (Peak Dose without SAV Correlations) (rem/yr)
Log (Peak Dose with SAV Correlations) (rem/yr)
Th-230
Ra-226
Pb-210
Pb-210
Ra-226
Th-230
Log (Peak Dose without SAV Correlations) (rem/yr)
Log (Peak Dose with SAV Correlations) (rem/yr)
Tc-99
I-129
Log (Peak Dose without SAV Correlations) (rem/yr)
Log (Peak Dose with SAV Correlations) (rem/yr)
Peak TEDE
(all nuclides)
Log (Peak Dose without SAV Correlations) (rem/yr)
Log (Peak Dose with SAV Correlations) (rem/yr)
Time to Peak TEDE
(all nuclides)
Time to Peak Dose without SAV Correlations (yr)
Time to Peak Dose with SAV Correlation (yr)

Figure 12

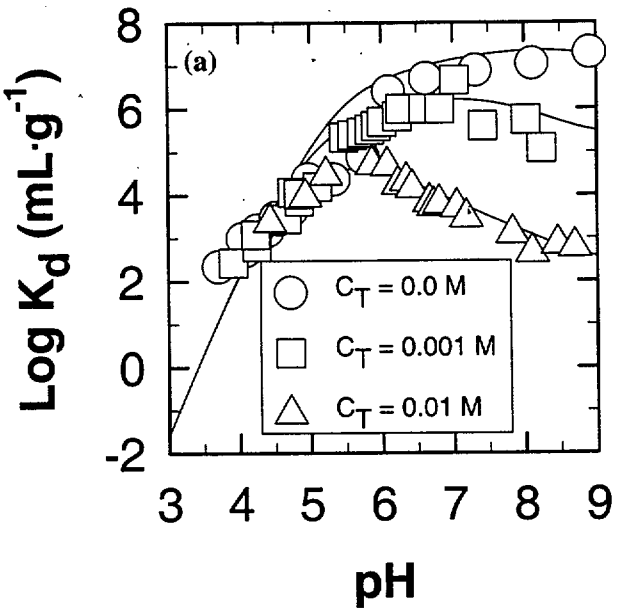
(a)
Log K_d (mL·g^{-1})
8
6
4
2
0
-2
3 4 5 6 7 8 9
pH
C_T = 0.0 M
C_T = 0.001 M
C_T = 0.01 M

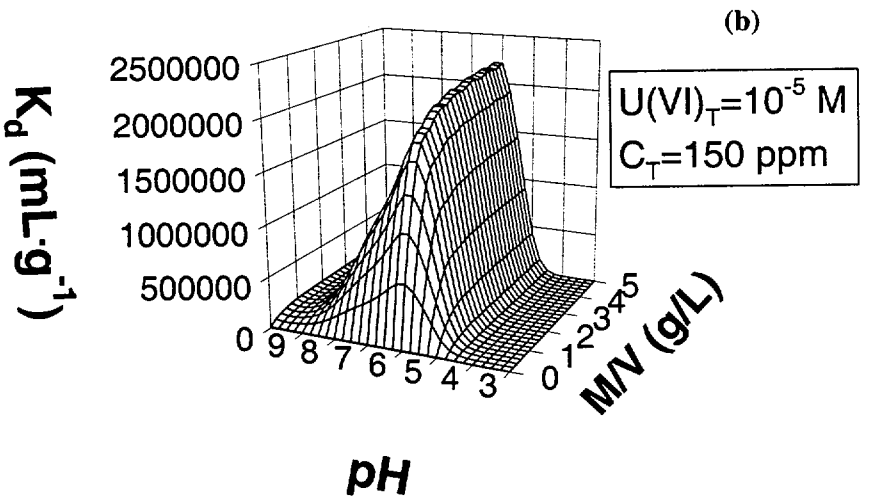
(b)
K_d (mL·g^{-1})
2500000
2000000
1500000
1000000
500000
0
9 8 7 6 5 4 3
pH
0 1 2 3 4 5
M/V (g/L)
U(VI)$_T$=10^{-5} M
C_T=150 ppm

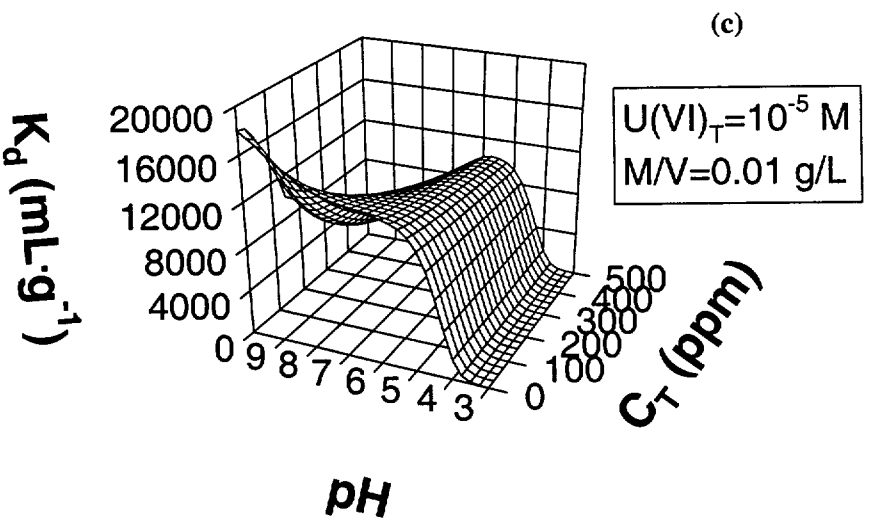
(c)
K_d (mL·g^{-1})
20000
16000
12000
8000
4000
0
9 8 7 6 5 4 3
pH
0 100 200 300 400 500
C_T (ppm)
U(VI)$_T$=10^{-5} M
M/V=0.01 g/L

Figure 13

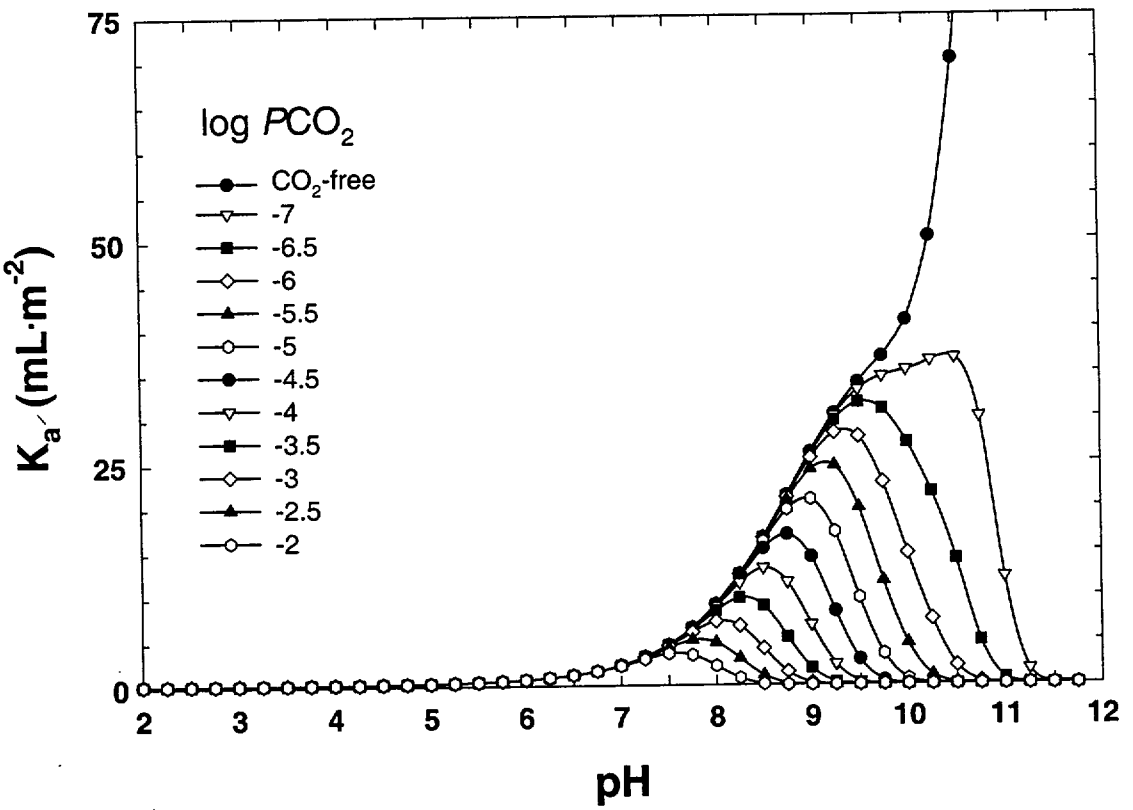
75
50
25
0
K_a (mL·m^{-2})
log PCO_2
CO_2-free
-7
-6.5
-6
-5.5
-5
-4.5
-4
-3.5
-3
-2.5
-2
2
3
4
5
6
7
8
9
10
11
12
pH

Figure 14

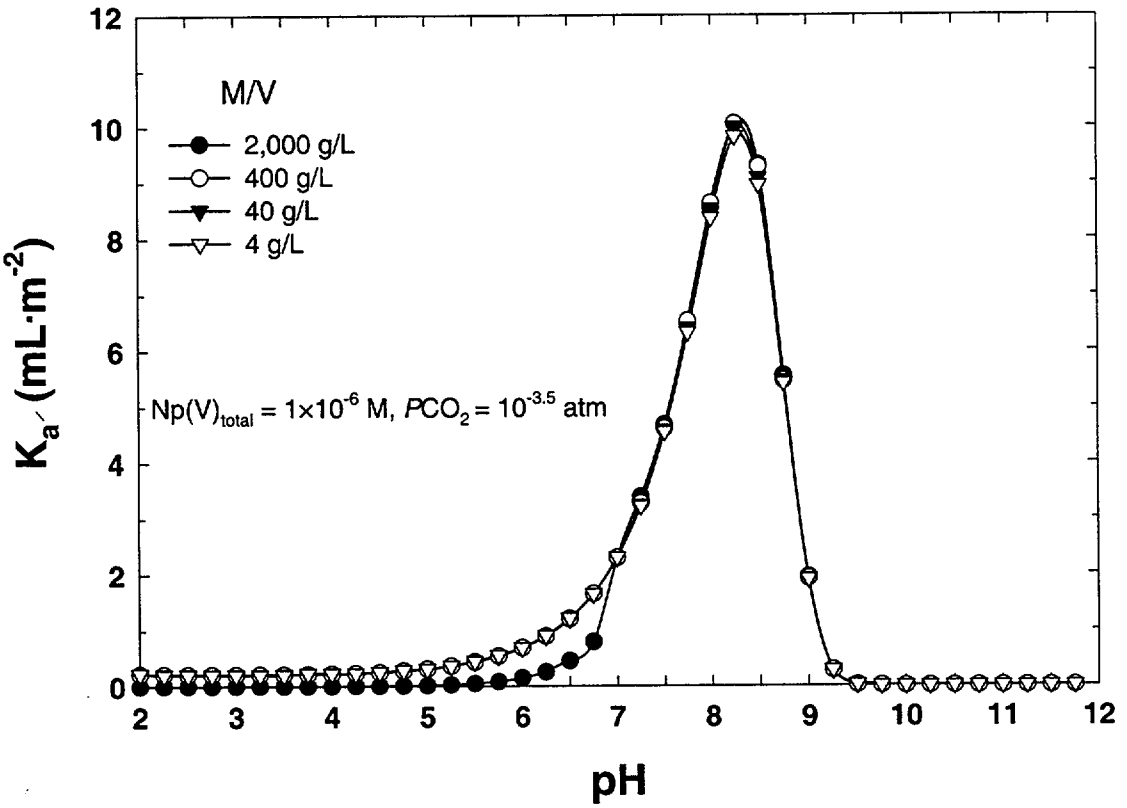
M/V
2,000 g/L
400 g/L
40 g/L
4 g/L
Np(V)total = 1×10-6 M, PCO2 = 10-3.5 atm
Ka' (mL·m-2)
pH
0
2
4
6
8
10
12
2
3
4
5
6
7
8
9
10
11
12

Figure 15

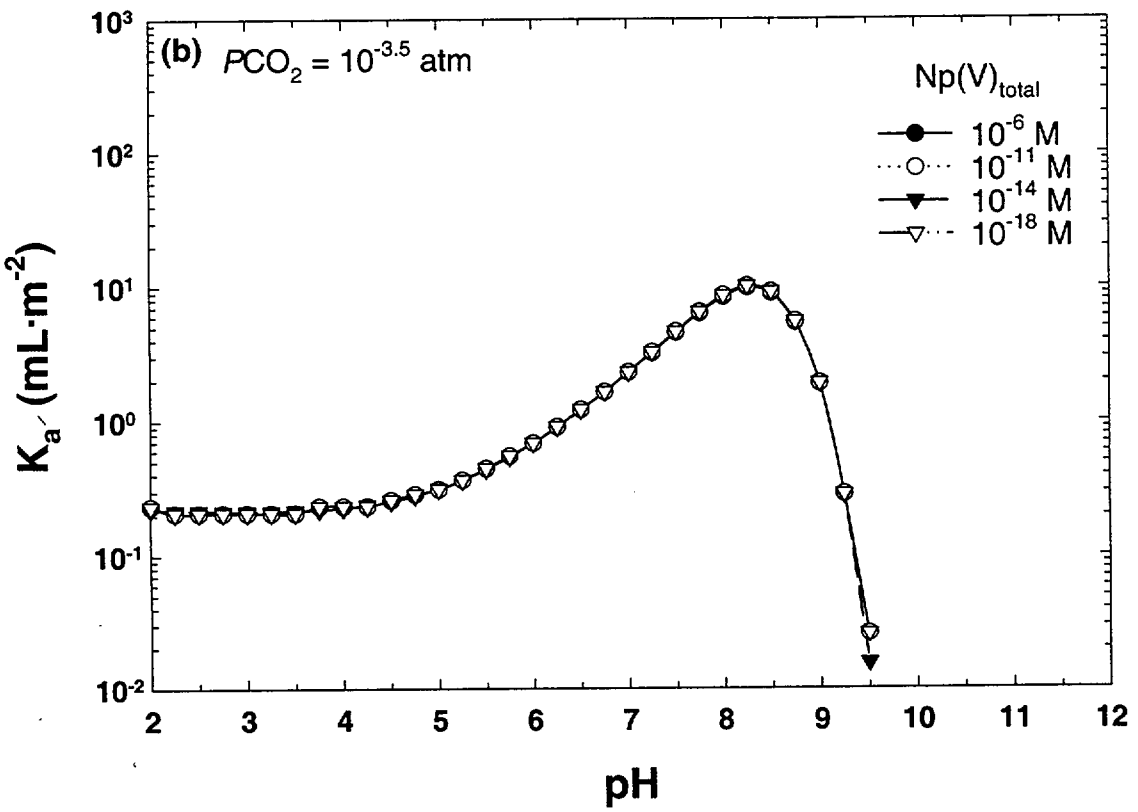
(b) $PCO_2 = 10^{-3.5}$ atm
$Np(V)_{total}$
10^{-6} M
10^{-11} M
10^{-14} M
10^{-18} M
$K_{a'}$ (mL·m^{-2})
10^{3}
10^{2}
10^{1}
10^{0}
10^{-1}
10^{-2}
2
3
4
5
6
7
8
9
10
11
12
pH

Figure 16

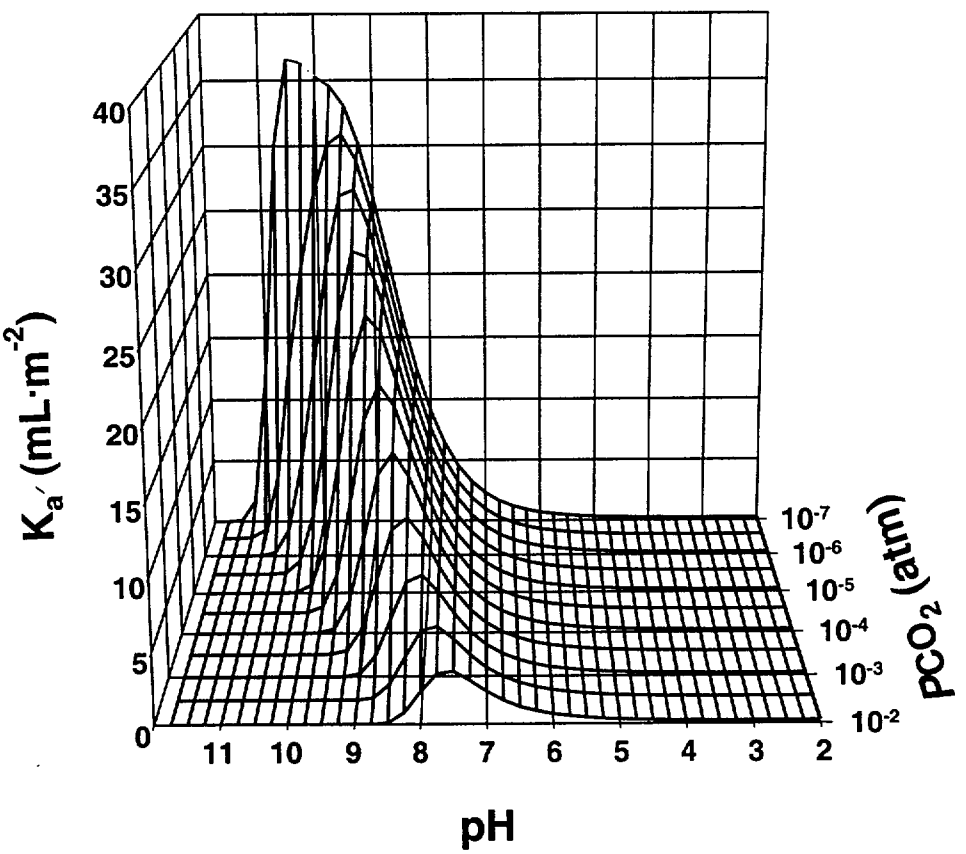
$K_{a'}$ (mL·m^{-2})
40
35
30
25
20
15
10
5
0
11
10
9
8
7
6
5
4
3
2
pH
10^{-7}
10^{-6}
10^{-5}
10^{-4}
10^{-3}
10^{-2}
PCO_2 (atm)

Figure 17

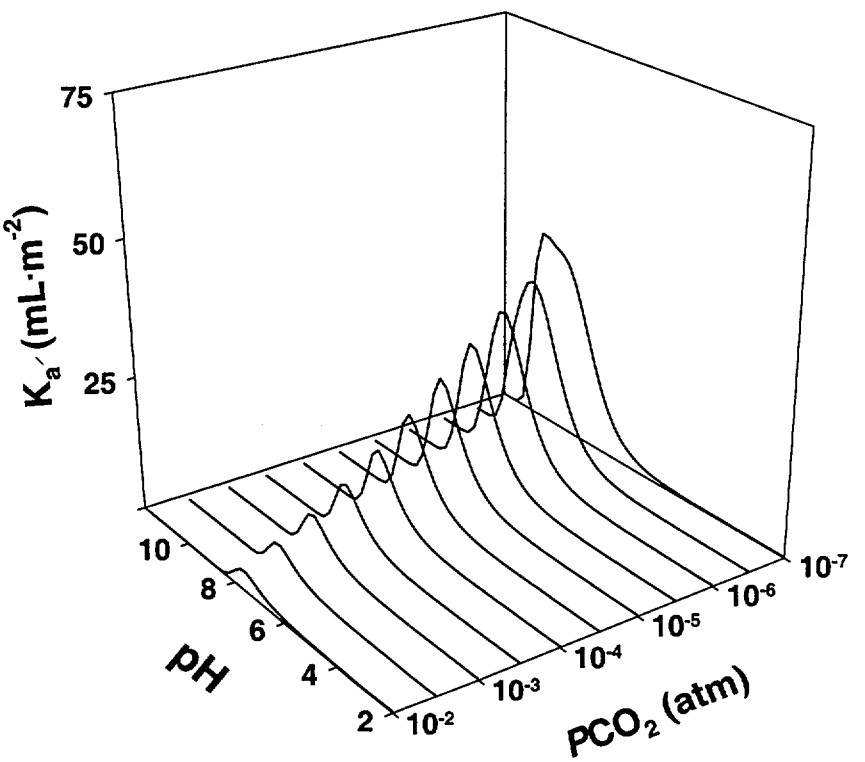

FIGURE 18

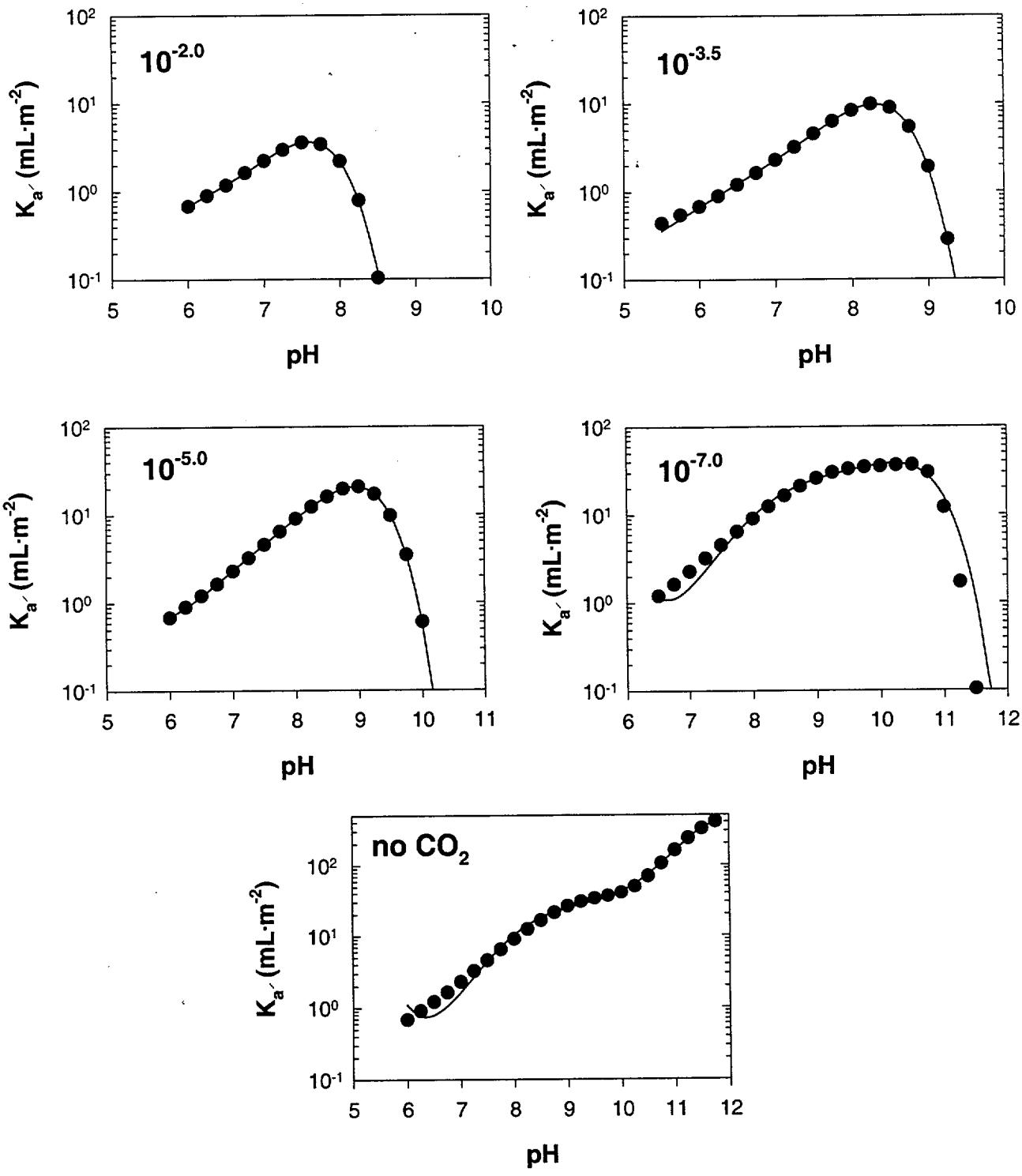

Figure 19

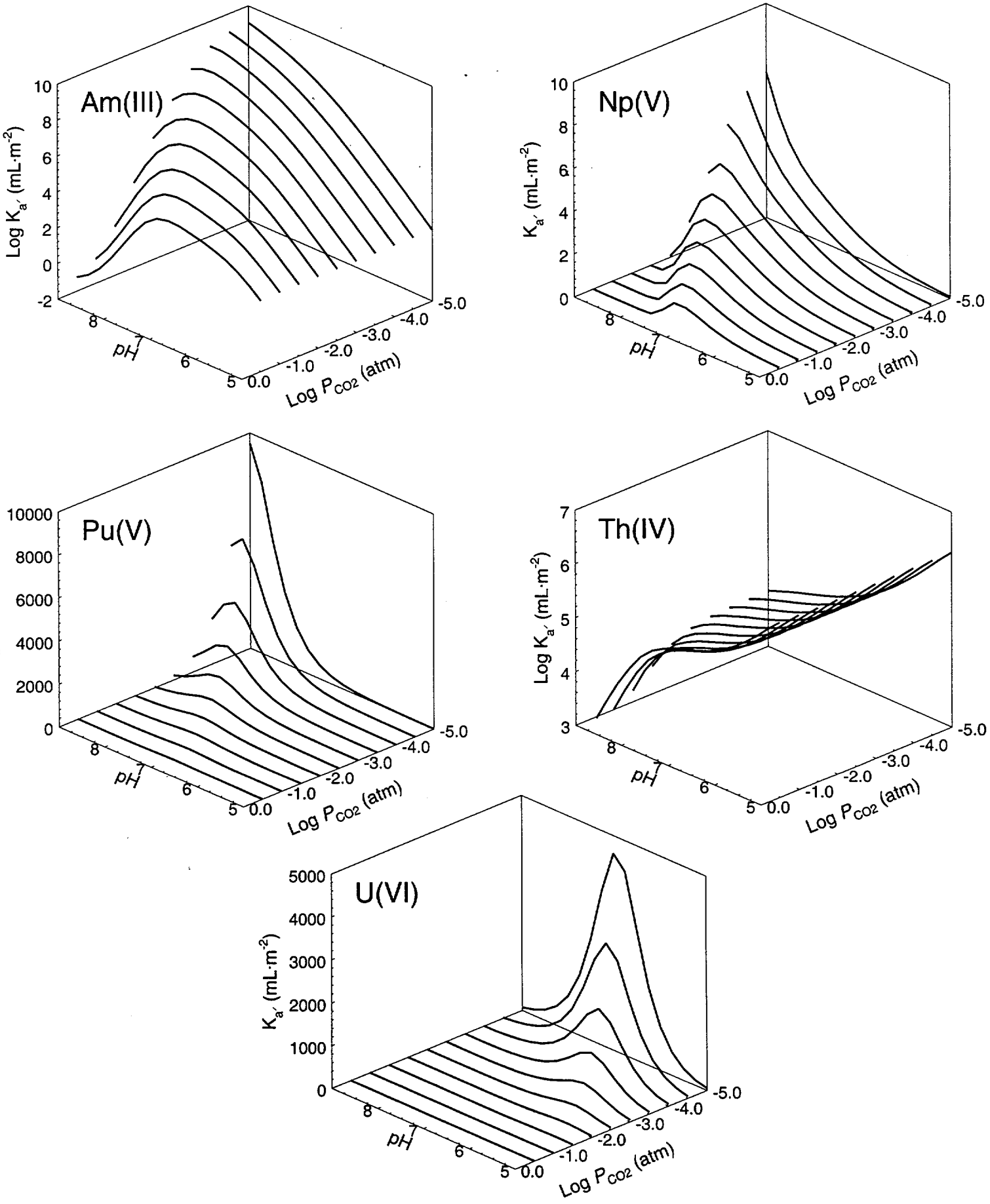
Am(III)
Log $K_{a'}$ (mL·m^{-2})
10
8
6
4
2
0
-2
pH
8
6
5
Log P_{CO2} (atm)
0.0
-1.0
-2.0
-3.0
-4.0
-5.0
Np(V)
$K_{a'}$ (mL·m^{-2})
10
8
6
4
2
0
pH
8
6
5
Log P_{CO2} (atm)
0.0
-1.0
-2.0
-3.0
-4.0
-5.0
Pu(V)
$K_{a'}$ (mL·m^{-2})
10000
8000
6000
4000
2000
0
pH
8
6
5
Log P_{CO2} (atm)
0.0
-1.0
-2.0
-3.0
-4.0
-5.0
Th(IV)
Log $K_{a'}$ (mL·m^{-2})
7
6
5
4
3
pH
8
6
5
Log P_{CO2} (atm)
0.0
-1.0
-2.0
-3.0
-4.0
-5.0
U(VI)
$K_{a'}$ (mL·m^{-2})
5000
4000
3000
2000
1000
0
pH
8
6
5
Log P_{CO2} (atm)
0.0
-1.0
-2.0
-3.0
-4.0
-5.0

Figure 20

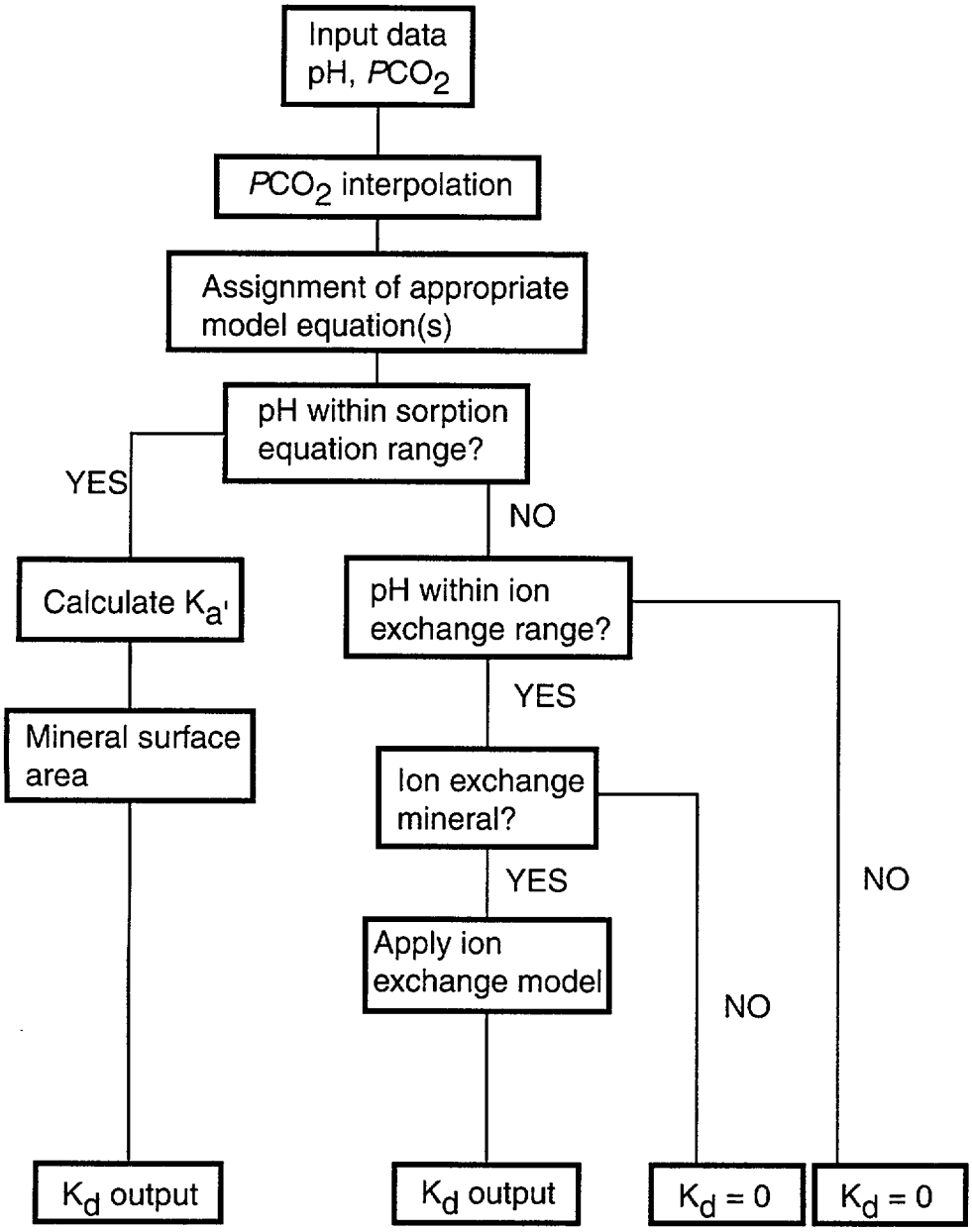
Input data
pH, PCO_2
PCO_2 interpolation
Assignment of appropriate model equation(s)
pH within sorption equation range?
YES
NO
Calculate $K_{a'}$
pH within ion exchange range?
Mineral surface area
YES
Ion exchange mineral?
YES
NO
Apply ion exchange model
NO
K_d output
K_d output
$K_d = 0$
$K_d = 0$